(1)

Report No. CG-D-05-94

AD-A279 527

# AIRCRAFT CORROSION STUDY



J.T. Stropki
and
R.D. Smith

Battelle
505 King Avenue
Columbus, Ohio 43201



FINAL REPORT
December 1993



Prepared for:

U.S. Coast Guard
Research and Development Center
1082 Shennecossett Road
Groton, Connecticut 06340-6096



and

U.S. Department Of Transportation
United States Coast Guard
Office of Engineering, Logistics, and Development
Washington, DC 20593-0001

# NOTICE

This document is disseminated under the sponsorship of the Department of Transportation in the interest of information exchange. The United States Government assumes no liability for its contents or use thereof.

The United States Government does not endorse products or manufacturers. Trade or manufacturers' names appear herein solely because they are considered essential to the object of this report.

The contents of this report reflect the views of the Coast Guard Research & Development Center. This report does not constitute a standard, specification, or regulation.


D. L. Motherway
Technical Director, Acting
United States Coast Guard
Research & Development Center
1082 Shennecossett Road
Groton, CT 06340-6096

Technical Report Documentation Page

| 1. Report No. | 2. Government Accession No. | 3. Recipient's Catalog No. |
|---|---|---|
| CG-D-05-94 | | |

| 4. Title and Subtitle | 5. Report Date |
|---|---|
| Aircraft Corrosion Study | December 1993 |
| | 6. Performing Organization Code |
| 7. Author(s) J.T. Stropki and R.D. Smith | 8. Performing Organization Report No. R&DC 01/94 |
| 9. Performing Organization Name and Address<br>Battelle<br>505 King Avenue<br>Columbus, OH 43201 | 10. Work Unit No. (TRAIS) |
| | 11. Contract or Grant No. F09603-90-D-2217/0004 |
| | 13. Type of Report and Period Covered Final Report |
| 12. Sponsoring Agency Name and Address<br>U.S. Coast Guard<br>Research and Development Center<br>1082 Shennecossett Road<br>Groton, Connecticut 06340-6096<br><br>Department of Transportation<br>U.S. Coast Guard<br>Office of Engineering, Logistics, and Development<br>Washington, D.C. 20593-0001 | 14. Sponsoring Agency Code |

15. Supplementary Notes
Coast Guard R&D Center COTR: Dr. Alan Bentz

16. Abstract

A comparison of the test results obtained for the unaged French and 2024-T3 (bare and hard anodized) alloys suggests that the resistance of all materials to raindrop erosion is identical. Superior performance of the hard anodized Alloy 2024-T3 sample was not observed during the erosion testing. Post-test examinations of the hard anodized 2024-T3 sample indicate that the performance of the coating was limited by spalling of the coating from the substrate. A review of the literature suggests that this condition is due to abnormal surface roughness of the anodic coating. This condition, which can be minimized with the application of silicone waxes ( or similar surface treatments) to the coated surfaces, does contribute to poor chemical and impact resistance. No pre-test surface characterizations were performed on this material.

In summary, the results of this program suggest that Alloy 2024-T3 be considered as a candidate replacement material for the French alloy that is currently being used on the outer wing slats of the HU-25A aircraft. The local overheating (retempering) of the material during anti-icing periods will reduce the corrosion and erosion-related performance of the alloy; however, the degradation will be no worse than currently being experienced with the French alloy. Additional testing of the hard anodized Alloy 2024-T3 is required before this material can be recommended over the uncoated material.

| 17. Key Words | 18. Distribution Statement |
|---|---|
| aircraft corrosion<br>outer wing slat | Document is available to the U.S. public through the National Technical Information Service, Springfield, Virginia 22161 |

| 19. Security Classif. (of this report) | 20. SECURITY CLASSIF. (of this page) | 21. No. of Pages | 22. Price |
|---|---|---|---|
| UNCLASSIFIED | UNCLASSIFIED | | |

Form DOT F 1700.7 (8/72) Reproduction of form and completed page is authorized

# METRIC CONVERSION FACTORS

## Approximate Conversions to Metric Measures

| Symbol | When You Know | Multiply By | To Find | Symbol |
|---|---|---|---|---|
| | | **LENGTH** | | |
| in | inches | * 2.5 | centimeters | cm |
| ft | feet | 30 | centimeters | cm |
| yd | yards | 0.9 | meters | m |
| mi | miles | 1.6 | kilometers | km |
| | | **AREA** | | |
| $in^2$ | square inches | 6.5 | square centimeters | $cm^2$ |
| $ft^2$ | square feet | 0.09 | square meters | $m^2$ |
| $yd^2$ | square yards | 0.8 | square meters | $m^2$ |
| $mi^2$ | square miles | 2.6 | square kilometers | $km^2$ |
| | acres | 0.4 | hectares | ha |
| | | **MASS (WEIGHT)** | | |
| oz | ounces | 28 | grams | g |
| lb | pounds | 0.45 | kilograms | kg |
| | short tons (2000 lb) | 0.9 | tonnes | t |
| | | **VOLUME** | | |
| tsp | teaspoons | 5 | milliliters | ml |
| tbsp | tablespoons | 15 | milliliters | ml |
| fl oz | fluid ounces | 30 | milliliters | ml |
| c | cups | 0.24 | liters | l |
| pt | pints | 0.47 | liters | l |
| qt | quarts | 0.95 | liters | l |
| gal | gallons | 3.8 | liters | l |
| $ft^3$ | cubic feet | 0.03 | cubic meters | $m^3$ |
| $yd^3$ | cubic yards | 0.76 | cubic meters | $m^3$ |
| | | **TEMPERATURE (EXACT)** | | |
| °F | Fahrenheit temperature | 5/9 (after subtracting 32) | Celsius temperature | °C |

*1 in = 2.54 (exactly).

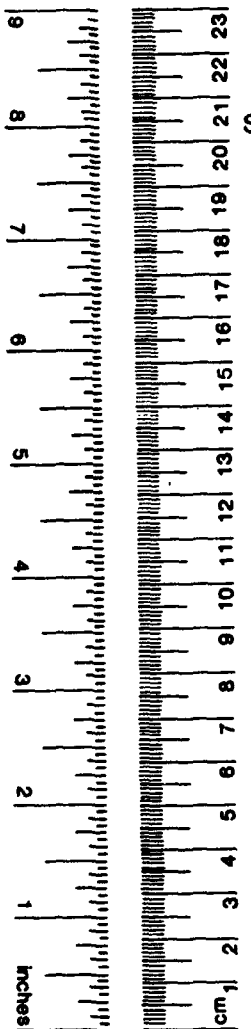


## Approximate Conversions from Metric Measures

| Symbol | When You Know | Multiply By | To Find | Symbol |
|---|---|---|---|---|
| | | **LENGTH** | | |
| mm | millimeters | 0.04 | inches | in |
| cm | centimeters | 0.4 | inches | in |
| m | meters | 3.3 | feet | ft |
| m | meters | 1.1 | yards | yd |
| km | kilometers | 0.6 | miles | mi |
| | | **AREA** | | |
| $cm^2$ | square centimeters | 0.16 | square inches | $in^2$ |
| $m^2$ | square meters | 1.2 | square yards | $yd^2$ |
| $km^2$ | square kilometers | 0.4 | square miles | $mi^2$ |
| ha | hectares (10,000 $m^2$) | 2.5 | acres | |
| | | **MASS (WEIGHT)** | | |
| g | grams | 0.035 | ounces | oz |
| kg | kilograms | 2.2 | pounds | lb |
| t | tonnes (1000 kg) | 1.1 | short tons | |
| | | **VOLUME** | | |
| ml | milliliters | 0.03 | fluid ounces | fl oz |
| l | liters | 0.125 | cups | c |
| l | liters | 2.1 | pints | pt |
| l | liters | 1.06 | quarts | qt |
| l | liters | 0.26 | gallons | gal |
| $m^3$ | cubic meters | 35 | cubic feet | $ft^3$ |
| $m^3$ | cubic meters | 1.3 | cubic yards | $yd^3$ |
| | | **TEMPERATURE (EXACT)** | | |
| °C | Celsius temperature | 9/5 (then add 32) | Fahrenheit temperature | °F |

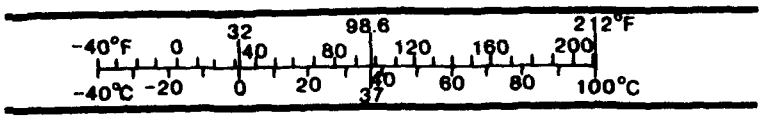

## Contents

## Contents (Continued)

## Contents (Continued)

Page

### Tables

## EXECUTIVE SUMMARY

This program was designed to determine the corrosion and erosion resistance of several aluminum alloys that are being used, or are being considered for use, in the "reskinning" of outer wing slats for the HU-25A Coast Guard aircraft. All material evaluations were accomplished through a series of controlled laboratory erosion and/or corrosion tests. An understanding of how the various alloys respond to the environmental conditions selected to simulate possible aircraft operations is required before the material(s) are accepted for use on the HU-25A aircraft.

The three aluminum alloys investigated during this program included a French alloy (aged and unaged), Alloy 2024-T3 (aged, unaged and hard anodized), and Alloy 2219-0 (aged and unaged). Representative samples of each alloy were tested in the "as-received" condition.

The test results indicate that Alloy 2219-0 should not be considered as a candidate replacement material for the outer wing slats of the HU-25A aircraft. The hardness, and therefore the erosion resistance, of this material is significantly less than that of the French and 2024-T3 alloys. This factor, combined with poor corrosion resistance of Alloy 2219-0, suggests that Alloy 2024-T3 be considered to replace the current French alloy.

Battelle also recommends the implementation of a suggestion by Falcon Jet personnel to incorporate a baffle into the center and/or inboard wing compartments of the HU-25A aircraft. During routine antiicing operations, this baffle(s) would serve to redirect the hot engine gases away from the current "hot spots" that are located along the leading edges of the outer wing slats. The results obtained from the erosion and corrosion testing of aluminum alloys that have been retempered to various temperatures indicate that the level of material degradation is controlled by temperature. Ideally, the temperature of the wing slat should not exceed 175°C.

Data obtained from the literature indicate that an eightfold reduction in corrosion-related damage on aircraft that are stationed in marine environments will occur if the aircraft are moved a minimum of 800 yards from the ocean. Some additional reductions in damage occur by moving aircraft up to about a mile from the coast, but no significant reductions occur at distances beyond one mile.

# INTRODUCTION

The United States Coast Guard aircraft operations create severe corrosion problems as a result of low-level flight profiles and parking in close proximity to marine environments. One of the specific questions being addressed in this study is whether there are more corrosion-resistant alloys that can be used to reskin the wing slats of Falcon jets.

One particular aircraft that receives a considerable amount of corrosion-related maintenance is the HU-25A Falcon jet. This aircraft is used by the Coast Guard for search and rescue and offshore surveillance, hence, its flight profile accelerates the potential for corrosion problems. Personnel from the Coast Guard Aircraft Repair Service Center (ARSC) located in Elizabeth City, N.C. have stated that more than fifty percent of the Falcon jet fleet have required wing corrosion repairs or maintenance. In most instances, the repairs are associated with the inboard and center wing slats which fail due to (1) the corrosive salt air and (2) thermal stresses induced as a result of the aircraft's wing anti-icing system.

The Falcon jet employs a wing anti-icing system that operates off hot air bled from the RH and LH engines. Distribution of the hot air to the leading edges of both wings is accomplished through two solenoid valves and a series of telescopic tubes that contain numerous holes. The activation of the system is electronically controlled by the pilot within the cockpit of the aircraft.

Local "hot spots" or areas of discoloration develop at specific locations along the leading edges of the inboard and center wing slats in response to a lack of venting of the hot air within the wing compartments. This condition is most severe when the slats are in the up position, which occurs when the aircraft is climbing and cruising. The wing deicers are used during these periods as well as when the aircraft is in inclement weather at high altitudes. However, it is not uncommon for the pilot to forget to turn the system off and leave the deicers running after the aircraft has landed. This additional exposure time contributes to a reduced service life of the inboard and center wing slats.

In an effort to reduce the costs and aircraft "down time" associated with premature wing slat failure, the U.S. Coast Guard is considering the replacement of the currently used French aluminum alloy with an alternative aluminum (Type 2024-T3 or 2219-0) alloy. As part of this consideration, the Coast Guard's Research and Development Center requested that Battelle conduct a program to perform (1) an analysis of a failed center slat fabricated from the French alloy, and (2) a chemical/physical characterization of the French and alternative aluminum alloys to quantify the corrosion and erosion resistance of each material. The results of all examinations and analyses obtained during this program are provided in this final report.

## OBJECTIVE

The objective of this program was to determine the corrosion and erosion resistance of several aluminum alloys that are being used or are being considered for use in the reskinning of wing slats for the HU-25A aircraft. All information obtained from the program will be used by the Coast Guard to select a material that increases the reliability and maintainability of the HU-25A aircraft.

## TECHNICAL APPROACH

The scope of this program included the following:

- An analysis on a small piece of failed wing slat removed from the leading edge of the center slat of an operational HU-25A Falcon jet. The slat was fabricated from the French alloy.
- A comparative evaluation of the corrosion and erosion resistance of the French aluminum alloy with its nominal American equivalent alloy (2024-T3), and comparison of the performance of both alloys with the Alloy 2219-0.
- A determination of the maximum temperatures reached on the leading edges of the center slats when the Falcon jet deicers are functioning. In addition, identify any "hot spots" that are present and/or may develop along the leading edges of the inboard, center, and outboard slats of the aircraft were to be identified.
- A literature search on "seafront exposure tests" that were performed using ASTM (American Society of Testing Methods) or other atmospheric testing methods. All data were evaluated on the basis of CG aircraft stationed on the ground in corrosive atmospheres or in low-level flight over salt water.

## EXPERIMENTAL PROCEDURES

The technical activities of this program were divided into four separate tasks. An abbreviated summary of the materials tested, experimental protocol, and all techniques used to analyze the results obtained during these tasks are provided in the following text for each of the tasks.

## Task 1. Alloy Evaluation

This task included a comparison of the American and French aluminum alloys that are used for the outer coating of HU-25A Falcon jet wing slats. Samples of used and new French alloys were included in the evaluation, as well as Alloys 2024-T3 and 2029-0. A listing of the quantity, size and "as-received" condition of the alloys investigated in this task is provided in Table 1.

**Table 1. Summary of aluminum alloys provided for testing in Task 1.**

| Quantity | Dimensions, in. | Aluminum Alloy | Surface Treatment |
|---|---|---|---|
| 2 | 2" x 4" | 2219-0 | Bare Aluminum Sheet |
| 2 | 4" x 4" | 2024-T3 | Chromic Anodized Sheet per MIL-A-8625 Type I |
| 2 | 4" x 4" | 2-24-T3 | Bare Aluminum Sheet |
| 1 | 4" x 4" | Fr. Alloy | Bare Aluminum LH OUTB Skin (MY2013750G01, SN: 130AT112F) Removed from MA's W/O No. 1076 |

The activities of this task included (1) a chemical analysis to determine the concentrations of the alloying elements in each of the alloys being investigated, (2) a metallographic and microhardness analysis of all alloys, and (3) an analysis of each alloy's inherent corrosion resistance as determined by two (DC-polarization and ASTM B-117-85 salt fog) laboratory corrosion tests.

## Task 2. Evaluation of Erosion Resistance

The goal of Task 2 was to investigate the erosion resistance of several aluminum alloys using a high-speed water droplet erosion device. Comparative-type evaluations were performed on alloys that were in both the new or unused and aged (artificially or on the aircraft) conditions. Artificial aging refers to thermal treatment as might be encountered in the antiicing process. A summary of the alloys and any metallurgical conditioning of the test samples prior to testing is provided in Table 2.

The centrifugal erosion device was calibrated to expose small samples of the individuals alloys to a set of conditions that replicated the actual flight patterns of an HU-25A aircraft. Deionized water droplets used in all

**Table 2. Summary of aluminum alloys erosion-tested in Task 2.**

| Aluminum Alloy | Test Condition of Sample | Source of Samples |
|---|---|---|
| French Alloy | Virgin (used as reference material throughout testing) | Coast Guard ARSC |
| | Artificially aged 24 hours at 204 C | |
| | Artificially aged 110 hours at 220 C | |
| | Naturally aged on aircraft 2131 | Metal Air Service |
| | Naturally aged on unidentified aircraft | Metal Air Service |
| | | |
| 2024-T3 Alloy | Virgin | Coast Guard R&D Center |
| | Artificially aged 24 hours at 204 C | |
| | | |
| 2024-T3 Alloy (Hard Anodized) | Virgin | Metal Air Service |
| | | |
| 2029-0 Alloy | Virgin | Coast Guard R&D Center |
| | Artificially aged 24 hours at 204 C | |

testing contained 500 ppm of salt (NaCl), which simulated the sea salt air. The impingement angle of the droplets impacting the samples was maintained at 90 degrees to the test surface of the sample. The velocity of the samples ranged between 280 and 300 mph, which represents the approximate cruising/patrol air speed of the aircraft at low (500 to 5000 feet) altitude. Testing was conducted in a vacuum chamber that was maintained at 20 Torr and 76 to 78°F. All erosion-related damage to the individual samples was assessed at 2.5 hour, 5 hour, 7.5 hour, 10 hour and 12.5 hour exposure intervals.

## Task 3. Wing Slat Temperature Evaluation

The activities of this task concentrated on determining the maximum temperatures reached along the leading edges of inboard and center wing slats on the HU-25A aircraft under normal antiicing conditions. The investigation

included the use of thin, non-reversible temperature labels that were affixed to the inside surfaces of the appropriate wing slats. A change in the color of one of the six indicating windows on a label indicates the maximum temperature reached on the surface of the metal surfaces during antiicing. Five separate eight-dot (eight discrete temperature ratings) temperature labels were installed on a center wing slat of a single HU-25A aircraft by ARSC personnel in Elizabeth City, N.C.

Information collected by the temperature monitors was used to determine the level of heating that occurs at several areas along a center wing slat during antiicing. The influence of the localized heating or retempering on the microstructure of the French alloy was also investigated. Metallographic analysis techniques were used to validate any transformation of the microstructure which may potentially reduce the alloy's inherent resistance to erosion and/or corrosion.

### Task 4. Literature Search

The purpose of Task 4 was to conduct a literature search on all pertinent seafront exposure testing conducted with each of the aluminum alloys investigated in this program. The search concentrated on atmospheric corrosion data for environments that include high temperature, high humidity, and a corrosive sea salt air.

All information collected during this task was used to determine the effects of distance from the ocean on the corrosion rates of the different aluminum alloys being used or being considered for use in the fabrication of HU-25A wing slats. The Coast Guard can use this information to establish whether additional atmospheric corrosion testing is required to verify the merit of stationing or parking of Coast Guard aircraft further inland.

## RESULTS AND DISCUSSION

### Task 1. Alloy Evaluation

#### Metallographic Evaluation

**Uncorroded Test Samples.** A metallographic evaluation of three of the four aluminum test samples being examined during this program was completed. Representative sections from each sample were mounted on edge in an epoxy material and polished using metallographic techniques. The polished surfaces were examined using a low-power microscope and photographed prior to being

etched. Photomicrographs documenting the polished and etched surfaces of the individual samples are provided in Figures 1 through 3.

Five separate microhardness measurements were made on the polished surfaces of each of the three samples and representative sections of an aged and unaged French alloy using a Knoop indenter and 500 gram load. The average hardnesses calculated for all samples are provided in Table 3.

**Table 3. Microhardness data for five aluminum test samples.**

| Sample ID | Alloy Identification | Average Knoop Hardness (500 g load) |
|---|---|---|
| 1 | 2024-T3 (ANODIZED) | 134 |
| 2 | 2024-T3 (BARE) | 137 |
| 3 | 2219-0 (BARE) | 47 |
| 4 | FRENCH ALLOY | 153 |
| 5 | FRENCH ALLOY (AGED) | 150.5 |

The microstructures and hardness values measured for Samples No. 1 and No. 2 (Alloy 2024-T3) were nominally equivalent. Average hardness values calculated for the samples were 134 (No. 1) and 137 (No. 2). Examination of the microstructures for both samples indicated that the size and distribution of large dark particles (insoluble $CuMgAl_2$, $Cu_2MnAl_{20}$, and $Cu_2FeAl_7$ compounds) within the grains was similar. An absence of $CuMgAl_2$ precipitates along the grain boundaries of either alloy indicates that both materials were correctly heat treated to the -T3 temper.

As shown in Figure 3, the microstructure for sample No. 3 (Alloy 2219-0) contained a large number of coarse intermetallic compounds. These compounds were uniformly dispersed throughout the individual grains of this alloy; that distribution contributes to this material's resistance to degradation by elevated temperatures. As expected from a comparison of mechanical properties, the average microhardness measured for this particular material was significantly lower than measurements obtained for the 2024-T3 and French alloys.

The microstructure of an "aged" French alloy that was removed from a wing slat of an HU-25A Falcon jet aircraft is provided in Figures 4a and 4b. Intergranular and exfoliation corrosion was evident along the internal surface of the sample. Metallographic examinations confirmed that the attack was concentrated beneath a primer coating applied to the internal surface of the wing slat. Battelle's ability to determine if the attack was induced as a

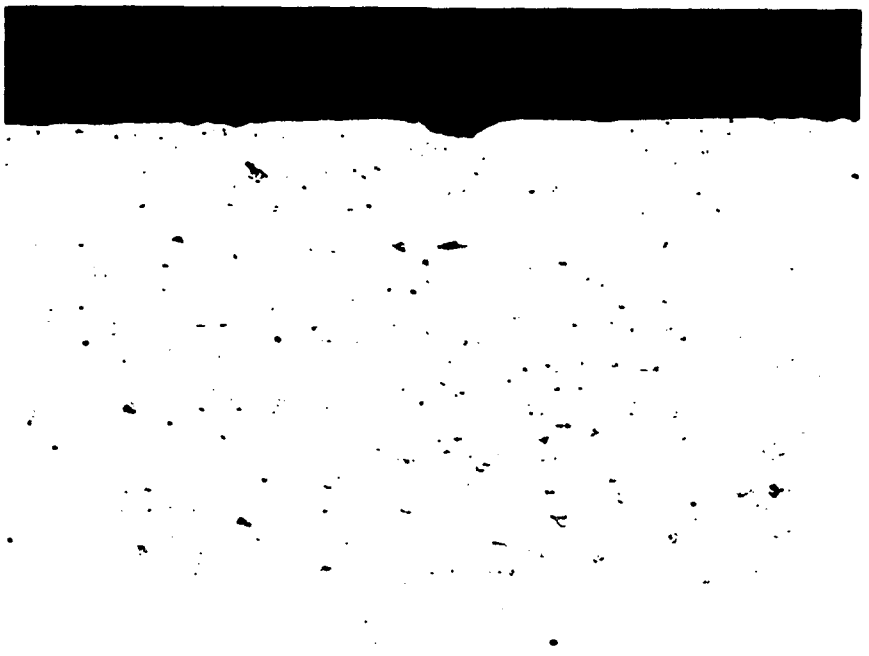

250X 50838

a. As Polished

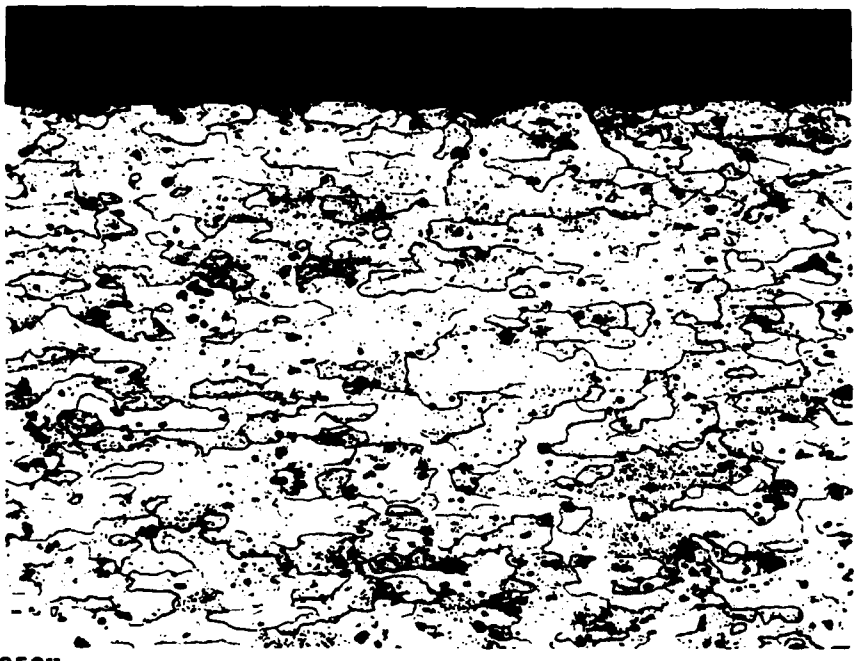

250X 50852

b. Etched

Figure 1. Photomicrographs documenting the microstructure of Specimen No. 1, Alloy 2024-T3 (Chromic Anodized per MIL-A-8625).

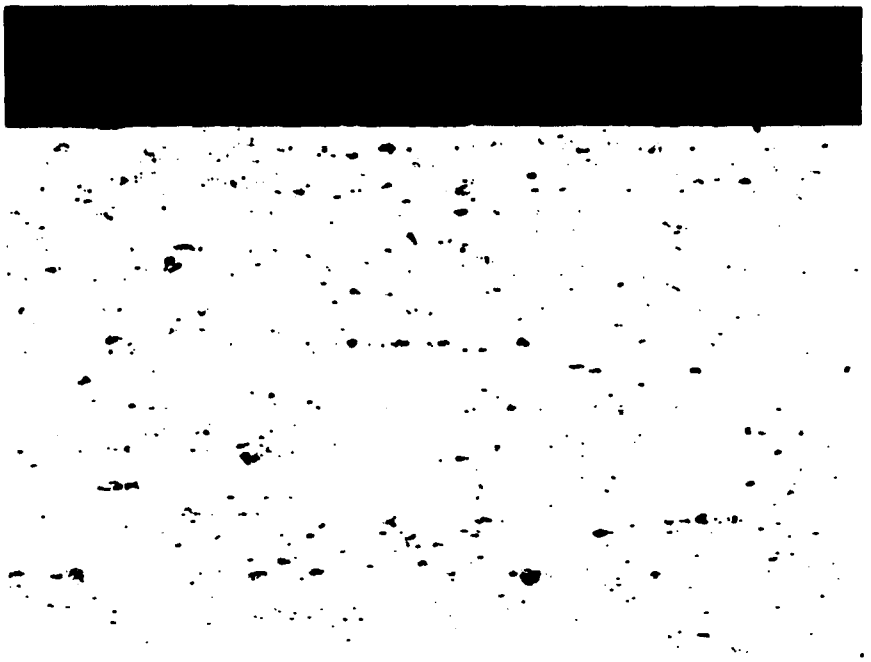

250X 50839

a. As Polished

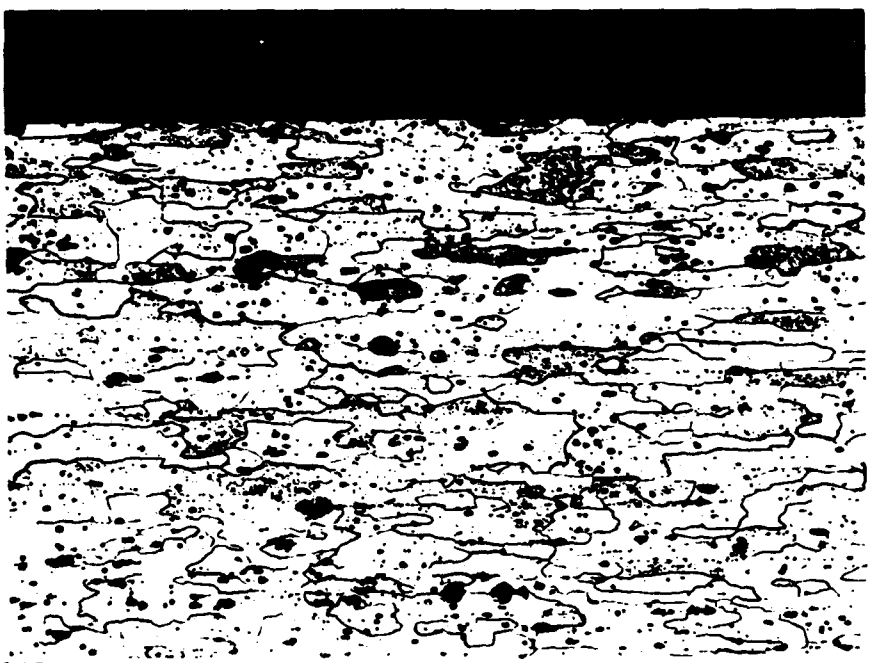

250X 50850

b. Etched

**Figure 2. Photomicrographs documenting the microstructure of Specimen No. 2, Alloy 2024-T3 (bare).**

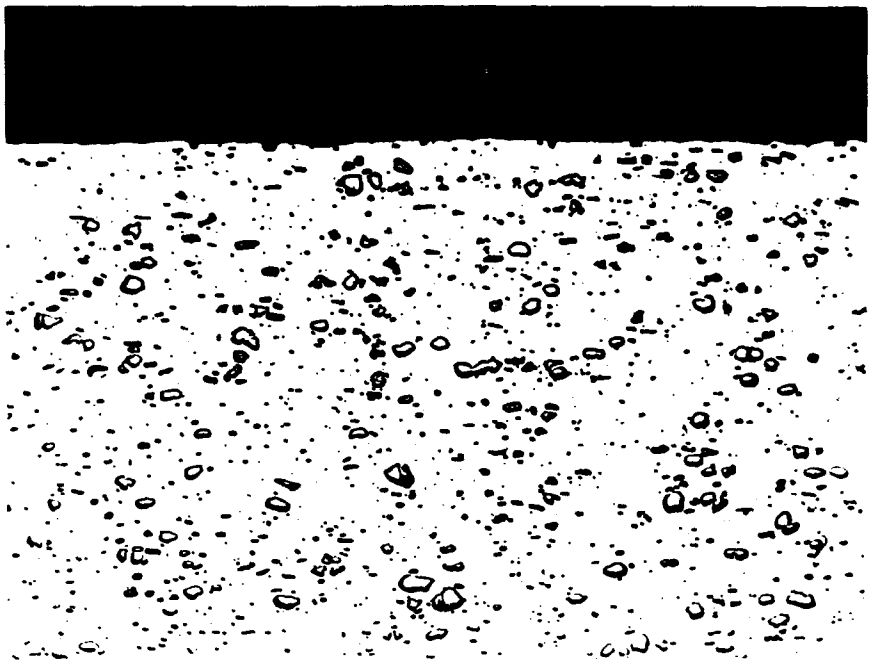

250X 50840

a. As Polished

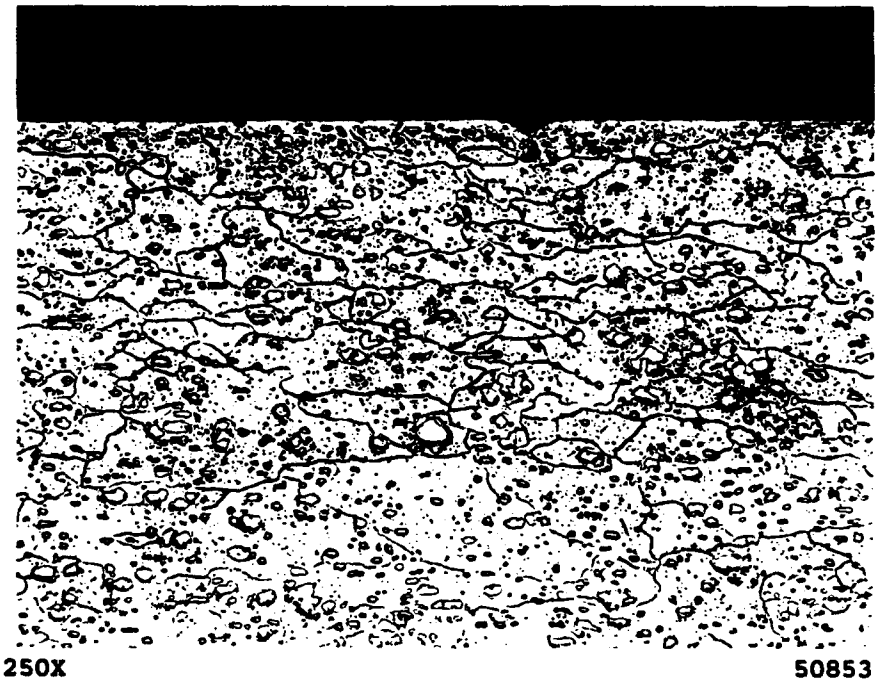

250X 50853

b. Etched

**Figure 3. Photomicrographs documenting the microstructure of Specimen No. 3, Alloy 2219-O (bare).**

250X 50841

a. As Polished

259X 50854

b. Etched

**Figure 4. Photomicrographs documenting the microstructure of Specimen No. 4, the French alloy (primed).**

result of (1) elevated temperatures (during antiicing of slat), (2) atmospheric corrosion, or (3) both, prior to being primed, was limited by a lack of service history on this particular component. No attack was noted along the external surfaces of the sample. As shown in Table 1, the average Knoop microhardness of this material was 153.

**Corroded Test Sample.** The metallographic examination of a small (1.0 inch by 1.0 inch) piece of eroded/corroded wing slat (see Figure 5) that was removed from an HU-25A aircraft (T/N 2131 - MY2014730G01 SN159F) was completed.

Photographs documenting the size and extent of corrosion attack on both the internal and external surfaces of the damaged wing slat sample are provided in Figure 6. The external surfaces of the "as-received" sample were analyzed using a stereomicroscope and scanning electron microscope (SEM). Energy Dispersive Spectroscopic analysis of x-rays (EDS) techniques were used to determine the semi-quantitative composition of the deposits contained within three distinct areas of the corroded sample. Those areas included one in a noncorroded region (Region A in Figure 6b), shown at higher magnification in Figure 7, and two within the corroded region surrounding the hole (Region B in Figure 6b), shown in higher magnification in Figure 8. The results of the EDS analyses are presented in Table 4.

**Table 4. Results of chemical analysis performed on corroded French alloy sample removed from HU-25A Aircraft.**

| Uncorroded Base Metal[a] | | Corroded Area A[b] | | Corroded Area B[b] | |
|---|---|---|---|---|---|
| Element | Wt. Percent[c] | Element | Wt. Percent[c] | Element | Wt. Percent[c] |
| Al | 78.1 | Al | 92.6 | Al | 97.1 |
| Si | 7.7 | Si | 0.6 | Si | 0 |
| P | 2.9 | P | 0 | P | 0 |
| S | 3.6 | S | 2.1 | S | 1.6 |
| Cl | 3.8 | Cl | 2.9 | Cl | 1.3 |
| K | 2.1 | K | 0.7 | K | 0 |
| Ca | 1.9 | Ca | 1.0 | Ca | 0 |

(a) See Figure 7.
(b) See Figure 8.
(c) Relative weight percent based upon the total number of counts of the elements detected.

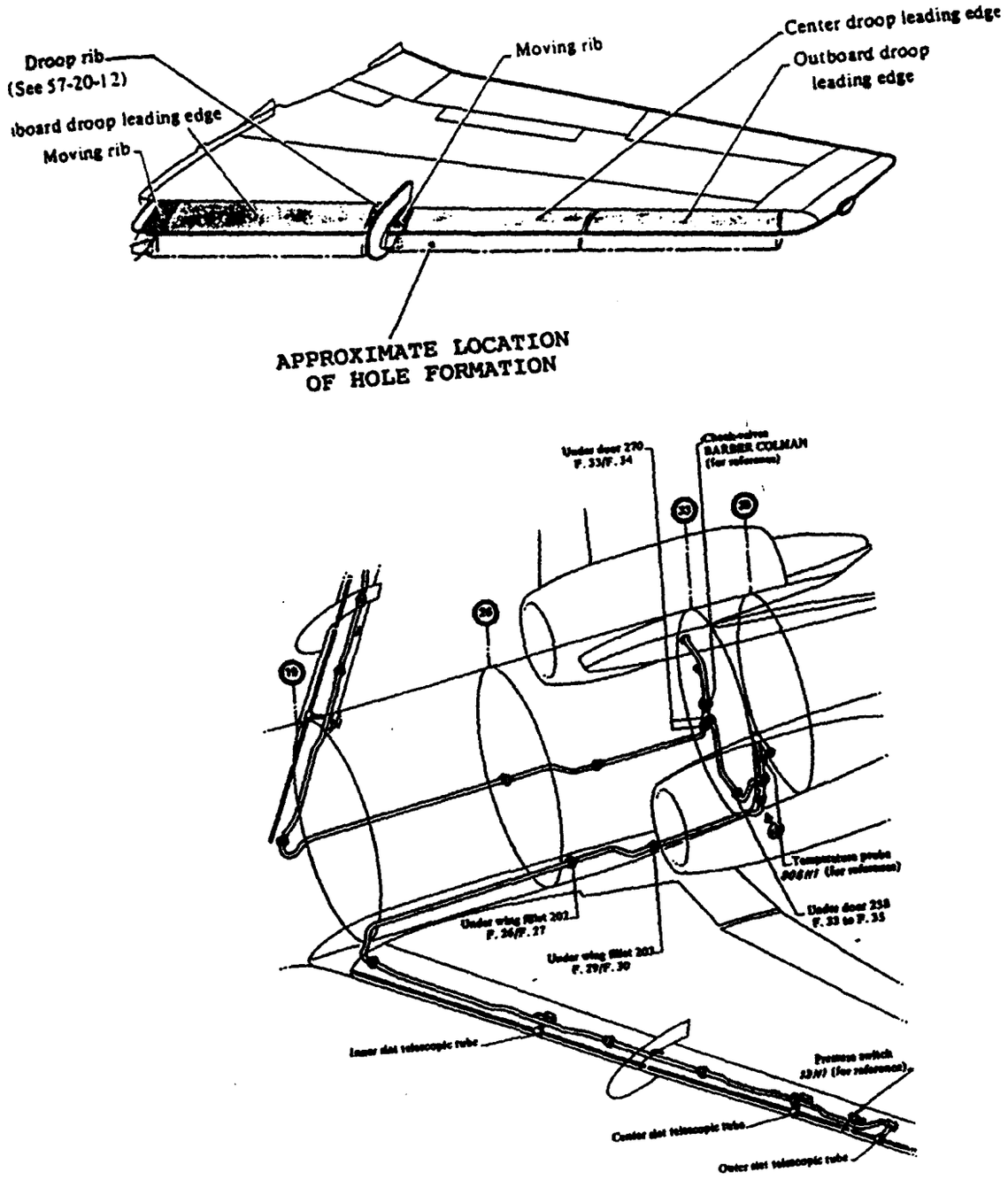


Figure 5. Diagrams of HU-25A RH wing documenting location of corroded slat and anti-icing tubes through inboard and center wing slats.

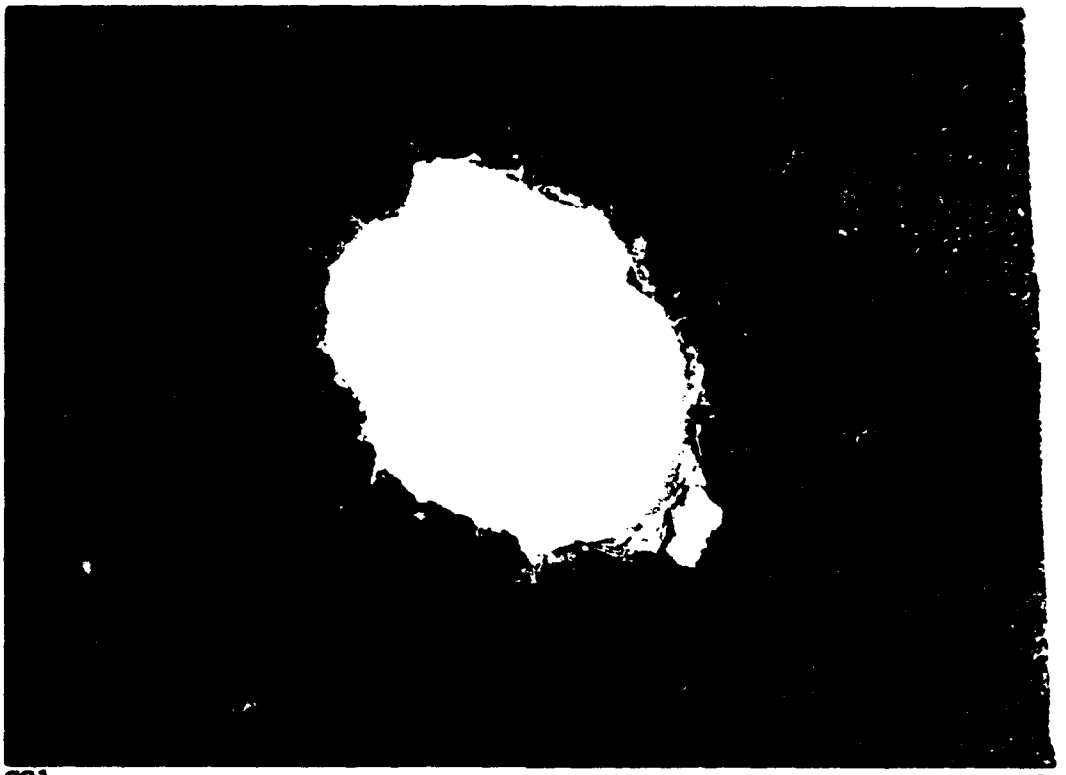

CG1 8X

a. Internal Surface

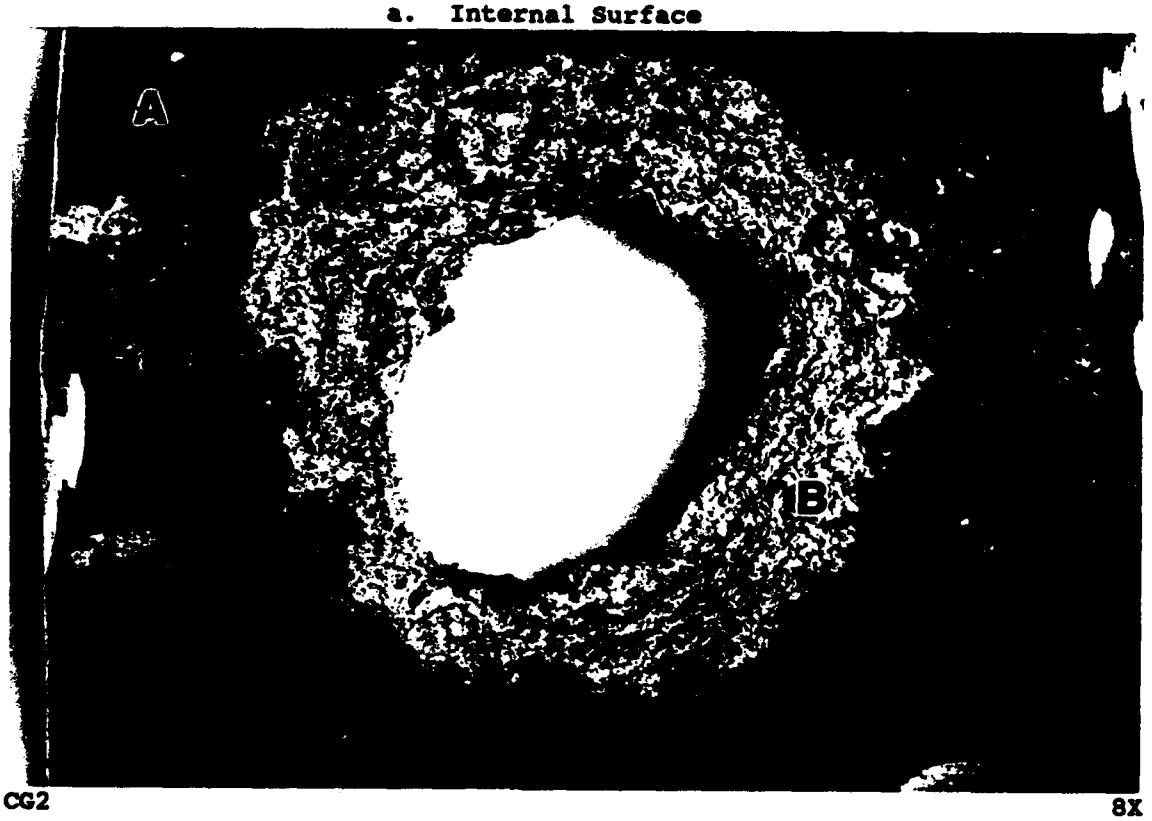


CG2 8X

b. External Surface

**Figure 6. Photographs documenting the extent of damage noted on the internal and external surfaces of a wing slat sample removed from an HU-25A aircraft.**

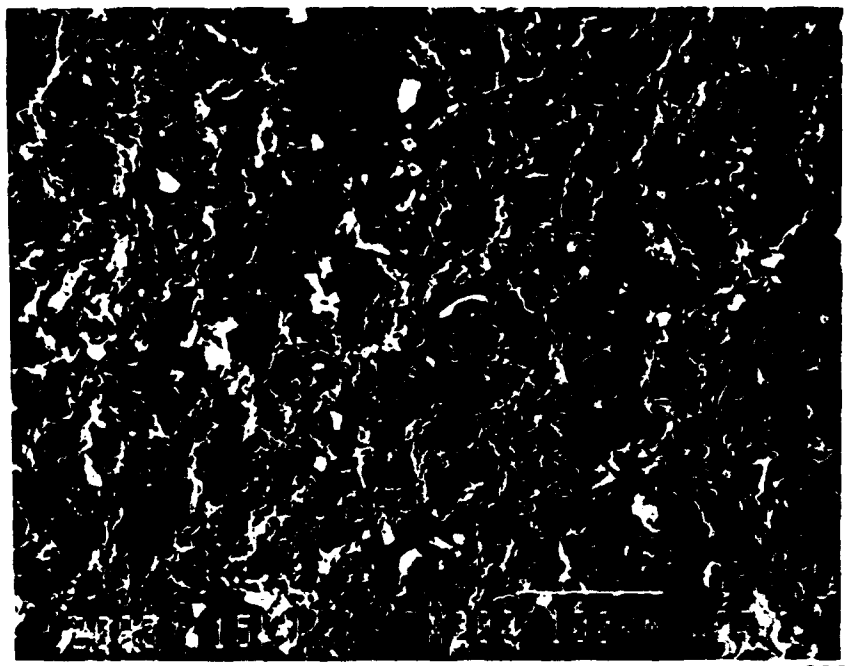

200X E2083

Figure 7. SEM photomicrograph illustrating the surface appearance and debris in Region A on Figure 6b on the external surface of the corroded wing slat sample removed from Aircraft T/N 2131.

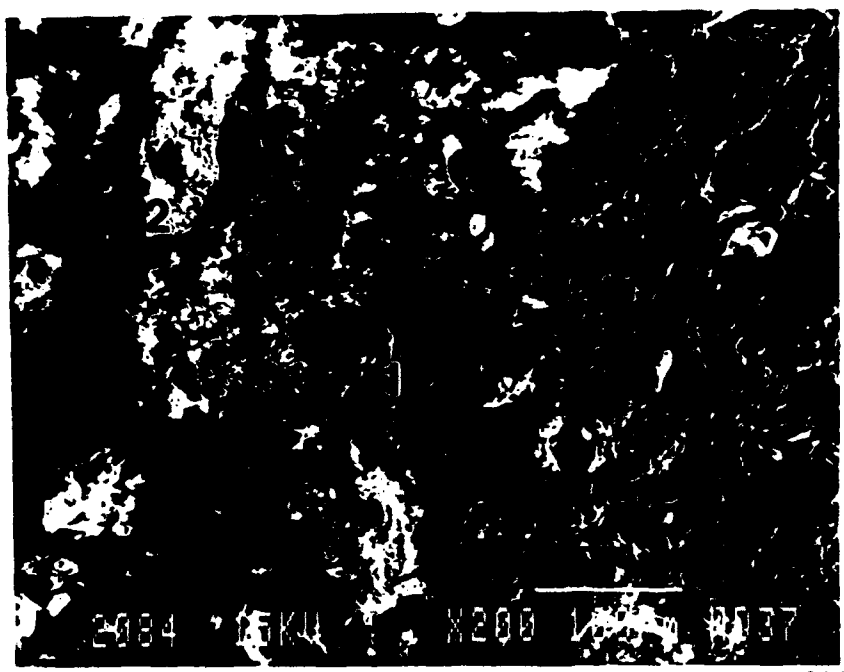


200X E2084

Figure 8. SEM photomicrograph illustrating corrosion damage and debris within two areas in Region B on Figure 6b of the sample removed from Aircraft T/N 2131

The numbers 1 and 2 are the regions in which EDS analyses were performed (see Table 2).

The results suggest high concentrations of silicon (Si), phosphorous (P), sulfur (S), chlorine (Cl), potassium (K), and calcium (Ca) on the uncorroded section of the sample. Conversations with Coast Guard personnel indicate that the suspected source of the silicon may be waxes that are periodically applied to the surfaces of the wings. Phosphorous, potassium, and calcium deposits may be attributed to the cleaners and/or aqueous rinses that are used to routinely clean the aircraft. Coastal mist and/or exhaust gas emissions are possible sources of the chlorine (chlorides) and sulfur (sulfates).

The concentration of all elements except sulfur and chlorine are low within the corroded sections of the wing slat sample. The presence of these elements on a susceptible aluminum material accelerates localized corrosion, as demonstrated by the magnitude of damage noted on the sample shown in Figure 6.

Additional processing of the damaged wing slat sample included mounting the entire sample in an epoxy material and selectively cutting the sample into four separate sections. Each section was then metallographically polished and etched for an examination of the sample's microstructure. Photomicrographs documenting the "as-polished" and "as-etched" condition of the alloy in two representative sections of the sample are shown in Figures 9a through 9d. An examination of each photomicrograph confirms the presence of severe intergranular and exfoliation corrosion. These failure modes are characteristic of the high strength aluminum materials, especially if the materials are overheated (retempered) and exposed to corrosive contaminants such as sulfates and chlorides.

**Chemical Analysis**

A single 2.0 inch by 2.0 inch sample was cut from four of the test samples (Alloys 2024-T3, 2219-0 and French alloy [aged and unaged]) being investigated in this task and forwarded to National Spectrographic Laboratories (NSL) for bulk chemical analysis. Standard quantitative spectroscopic analysis techniques were employed to determine the chemical composition of the samples.

NSL was instructed to analyze the three samples for the following nine elements: aluminum (Al), copper (Cu), manganese (Mn), magnesium (Mg), silicon (Si), chromium (Cr), zinc (Zn), nickel (Ni), and iron (Fe). The results of the analyses are summarized in Table 5.

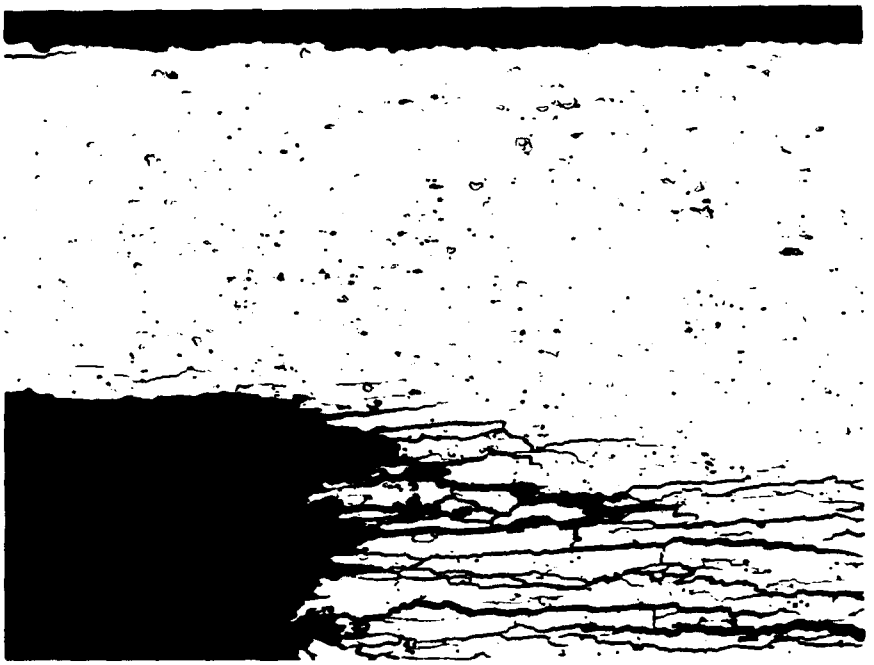


a. Area 1 (As-Polished)


b. Area 1 (Etched)

**Figure 9. Photomicrographs documenting the intergranular and exfoliation corrosion attack noted in two separate metallographic cross-sections taken through two areas of the damaged wing slat sample.**

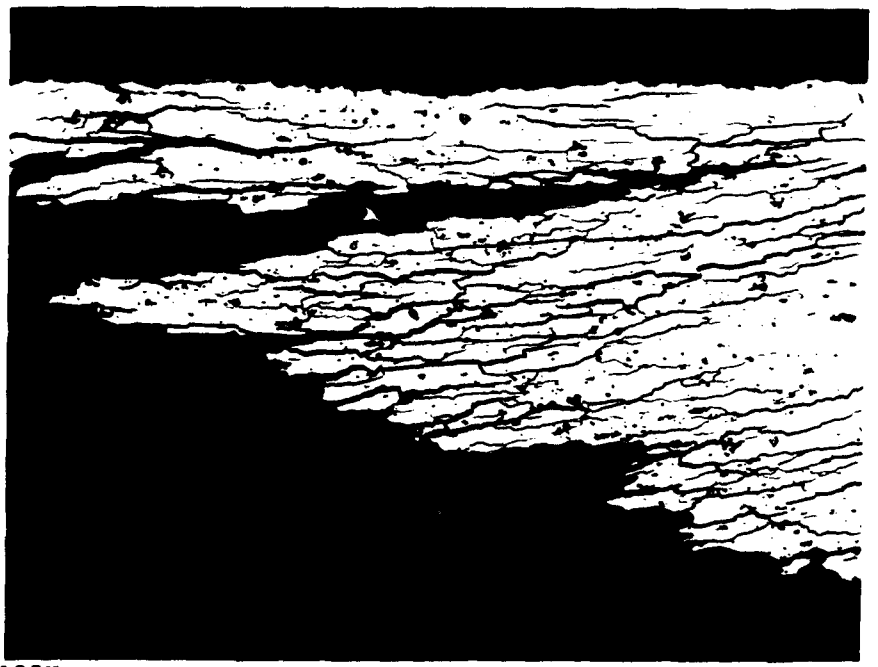

100X 50844

c. Area 2 (As-Polished)

250X 50857

d. Area 2 (Etched)

**Figure 9. (Continued)**

Table 5. Results of chemical analysis performed on four aluminum test samples.

| Sample Identification | Chemical Composition, weight percent | | | | | | | | |
|---|---|---|---|---|---|---|---|---|---|
| | Cu | Mn | Mg | Si | Cr | Zn | Ni | Fe | Al |
| 2024-T3 | 3.98 | 0.49 | 1.45 | 0.06 | <.05 | 0.06 | <.05 | 0.32 | rem |
| 2219-0 | 5.98 | 0.36 | 0.01 | 0.05 | <.05 | 0.05 | <.05 | 0.14 | rem |
| French Alloy (unaged) | 4.55 | 0.68 | 1.59 | 0.10 | <.05 | 0.12 | <.05 | 0.22 | rem |
| French Alloy (aged) | 4.28 | 0.75 | 1.52 | 0.12 | <.05 | 0.07 | <.05 | 0.30 | rem |

An examination of the data in Table 5 indicates that the concentrations of the alloying elements in the Alloy 2024-T3 and Alloy 2219-0 samples are consistent with the specifications listed in the ASM Handbook (Vol. 2, 10th Edition, 1990). In addition, the 2024-T3 and French alloy were shown to have similar chemical compositions, but the French alloy contained higher concentrations of copper, manganese, and silicon. However, the higher concentrations of those elements in the French alloy were within the specified ranges for the elements in Alloy 2024. A lack of additional information on the French alloy makes any further comparisons between this sample and the Alloy 2024-T3 sample difficult at this time.

A representative sample of a "new" or unaged piece of French alloy was received from the Metal Air Corporation and submitted to NSL for chemical analysis. This sample was obtained directly from the Falcon Jet Corporation in France; therefore, the sample was not environmentally aged on an operational aircraft. Information related to any heat treatment of the sample was not provided to Battelle. Comparisons among the data obtained for this sample and the "aged" French alloy sample indicate that the chemical compositions of both samples were similar. Additionally, the compositions of both samples met the requirements for Alloy 2024.

## Corrosion Tests

**Salt-Fog Test.** Conversations with Dr. Bentz of the Coast Guard's R&D Center resulted in the selection of two distinct aging conditions that were implemented during the testing performed in this task. In addition, Battelle recommended that a third aging procedure be included in the matrix to ascertain the effects of numerous heating and cooling cycles on the microstructure of the aluminum alloys. A listing of the conditions that were

used to artificially age the alloys tested in the ASTM B117-85 salt fog chamber are summarized as follows:

- Condition No. 1
  - Heat specimens to 149°C for 24 hours,
  - Air cool to room temperature

- Condition No. 2
  - Heat specimens to 246°C for 12 hours,
  - Air cool to room temperature

- Condition No. 3
  - Heat specimens to 149°C for 4 hours,
  - Air cool to room temperature,
  - Repeat cycle two additional times

Metallographic examinations were used to characterize the pre-exposure and post-exposure microstructures and hardnesses of all materials before and after heat treatment. A direct comparison between the microstructure of the French alloy samples that were artificially aged using each of three conditions and the sample that was aged on the Falcon Jet aircraft was performed prior to initiating any salt fog testing. The results of these comparisons indicated that there was a significant difference between the specimens aged at 149°C and 246°C; however, a minimal difference was observed between the two specimens aged at 149°C. The microstructures of the latter specimens were identical and very similar to the microstructure observed for the naturally aged specimen that was removed from a section of a damaged HU-25A wing slat.

The raw weight-loss data, as well as the corrosion rates that were calculated for each set of samples tested during this task are provided in Table 6. Photographs documenting the post-test, uncleaned condition of all samples are provided in Appendix A. Analysis of these data and the microscopic examinations performed on the exposed surfaces of each test coupon suggests that all three aging conditions of the French alloy had a high degree of corrosion resistance to the ASTM B117-85 salt fog test environment. As measured, the differences among the three sets of data were statistically insignificant and it is concluded that the inherent corrosion resistance of this particular material is not noticeably affected by thermal aging processes. This statement supports the premise that the damage noted at a single location on the center wing slat of the HU-25A aircraft is controlled

**Table 6. Results of salt fog corrosion test.**

| Material | Heat Treatment | Initial Weight, grams | Final Weight, grams | Delta Weight, grams | Corrosion Rate, (mils/yr) |
|---|---|---|---|---|---|
| French Alloy | Condition 1 | 2.8767<br>2.8245 | 2.8671<br>2.8104 | 0.0096<br>0.0141 | 5.51632<br>8.1021 |
| | Condition 2 | 2.7409<br>2.7713 | 2.7303<br>2.7602 | 0.0106<br>0.0111 | 6.09094<br>6.37825 |
| | Condition 3 | 2.7855<br>2.7513 | 2.7756<br>2.7411 | 0.0099<br>0.0102 | 5.68871<br>5.86109 |
| Alloy 2219 | Condition 1 | 3.3389<br>3.3292 | 3.3105<br>3.2893 | 0.0284<br>0.0399 | 15.6981<br>22.0547 |
| | Condition 2 | 3.2071<br>3.4305 | 3.1692<br>3.3984 | 0.0379<br>0.0321 | 20.9492<br>17.7432 |
| | Condition 3 | 3.0674<br>3.4447 | 3.0336<br>3.4143 | 0.0311<br>0.0304 | 17.1905<br>16.8036 |
| Bare 2024-T3 | Condition 1 | 3.7508<br>3.2996 | 3.7239<br>3.2754 | 0.0269<br>0.0242 | 15.4572<br>13.9057 |
| | Condition 2 | 3.6178<br>3.4809 | 3.5949<br>3.4647 | 0.0229<br>0.0162 | 13.1587<br>9.30879 |
| | Condition 3 | 3.4106<br>3.5288 | 3.3903<br>3.4995 | 0.0203<br>0.0293 | 11.6647<br>16.8363 |
| Chromated 2024-T3 | Condition 1 | 3.3107<br>3.4532 | 3.2999<br>3.4417 | 0.0108<br>0.0115 | 6.20586<br>6.60809 |
| | Condition 2 | 3.4943<br>3.3126 | 3.4815<br>3.2959 | 0.0128<br>0.0167 | 7.3551<br>9.5961 |
| | Condition 3 | 3.5171<br>3.1951 | 3.4994<br>3.1744 | 0.0177<br>0.0207 | 10.1707<br>11.8946 |

Notes: Condition 1 - 300°F for 24 hours
Condition 2 - 475°F for 12 hours
Condition 3 - 300°F for 4 hours (3 cycles)
mils/yr - mils of metal wastage per year

by both erosion and corrosion, rather than by microstructural variations in the material.

As shown in Table 6, the data collected for the two Alloy 2024-T3 samples (bare and chromated) indicates that the chromate conversion coating which was applied to the exposed surfaces of the tested samples affords some level of protection to the material. A determination of the extent and causes of degradation to this material was not within the scope of this program. However, the data indicate that each of the artificial aging processes affects the integrity of the coating, as the corrosion resistance of the material varies for the different heat treatments. The cyclic reheating (retempering) of the samples that were heated in three 4-hour intervals appears to influence the corrosion resistance of this material when compared to the samples that were continuously heated for 24 hours at 149°C.

All three sets of Alloy 2219-0 samples performed poorly in the salt fog corrosion test. The effects of the three heat treatments are not apparent in the weight loss data that were collected from all samples. Metallographic cross-sectional analysis techniques were used to characterize the extent of corrosion-related damage done to the microstructure of these specimens and each of the other sets of specimens that were tested during this task. These analyses and the results of post-test microscopic examinations performed on the tested surfaces of the samples indicate that the primary mode of attack to each sample was pitting and intergranular corrosion. The morphology and magnitude of attack was controlled by the (1) type of aluminum alloy, and (2) the microstructural transformations that occurred as a result of the various retempering treatments. Increased susceptibility to corrosion damage was attributed to a precipitation of $CuAl_2$ and $Al_xCu_xMg$ compounds along the grain boundaries.

**Electrochemical Polarisation Test.** A total of four DC polarization tests were performed during this task. All instrumentation was calibrated and the individual samples were prepared in accordance with the procedures referenced in ASTM G59-78. The test solution used to conduct each test was prepared in accordance with ASTM D1384. Tests were performed in this solution to determine the susceptibility of pitting for each of the four aluminum alloys defined in the previous text.

Pitting potential, i.e., the potential at which the passive film of a material begins to break down locally, is one of the most important features characterizing the susceptibility of an aluminum alloy to pitting corrosion. The procedure used in this program to determine the pitting potentials of each alloy involved a measurement of the anodic polarization curves for the individual alloys. By using potentiodynamic methods, all changes in current

density with potential were measured upward (negative to positive) from the corrosion potential of the respective alloy, and then backward to the corrosion potential. Two characteristic potentials that were then identified on each curve included (1) $E_{np}$, the potential at which a sudden increase of the current caused by pit nucleation on the surface of the test sample occurs, and (2) $E_{pp}$, the potential associated with a decrease in current caused by the repassivation of pits.

Figures 10a through 10d document the anodic polarization curves obtained for the four aluminum alloys after testing in ASTM D1384. An analysis of each curve indicates that Alloy 2024-T3 ($E_{np}$ = -285 mV) and the French alloy ($E_{np}$ = -300/-285 mV) are the most resistant to pitting corrosion. Conversely, the pitting potential measured for the anodized Alloy 2024-T3 sample was approximately -390 mV. The suspected source of this worse-than-expected result may be attributed to the quality of the protective anodized film on the surface of the test sample. Any scratches or discontinuities in the film would result in a decrease in corrosion resistance and an increased susceptibility to pitting corrosion.

The polarization behavior of Alloy 2219-0 indicates that this particular material is much more susceptible to localized corrosion attack than are the other three alloys that were examined by this testing method.

### Task 2. Evaluation of Erosion Resistance

The vacuum chamber within which the test samples were impacted is shown in Figure 11. In this chamber, two 0.5-inch by 0.5-inch by 0.0625-inch samples were attached 180 degrees from one another on a 5.75-inch OD by 0.5-inch-thick aluminum disc and rotated at 280 to 300 mph. Figure 12 documents the size and shape of the disc as well as the positioning of the individual samples on the disc. Preliminary calibration runs verified that no abnormally high stresses were introduced onto the holder as a result of the samples protruding from the edge of the disc. As shown in Figure 13, a single 0.25-inch hole was drilled into each sample to permit attachment to the disc. All samples were positioned on the disc so that the center of the sample was 6.0 inches from the axis of rotation. This design allowed for an excellent static and dynamic balance of the disc.

The disc was rotated by means of a high-speed 0.75-hp motor mounted outside the chamber, turning the shaft through a rotatable vacuum feedthrough. Minimal problems were encountered in the design of the bearings in this feedthrough.

The method used for generating drops with precisely controlled size relies on the Rayleigh instability which occurs in a liquid jet brought about

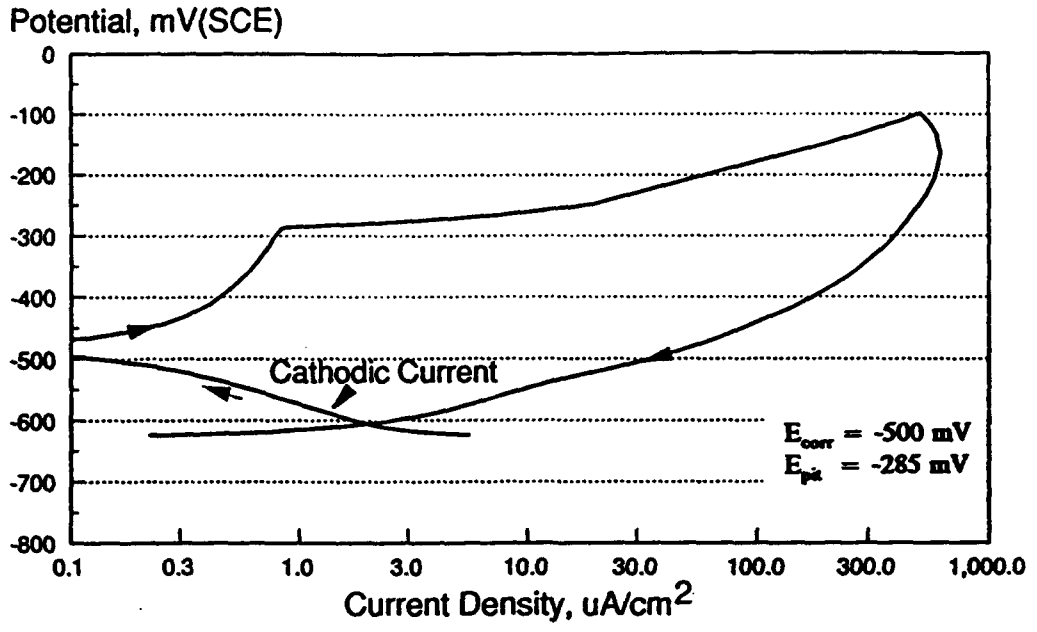


a. Alloy 2024-T3

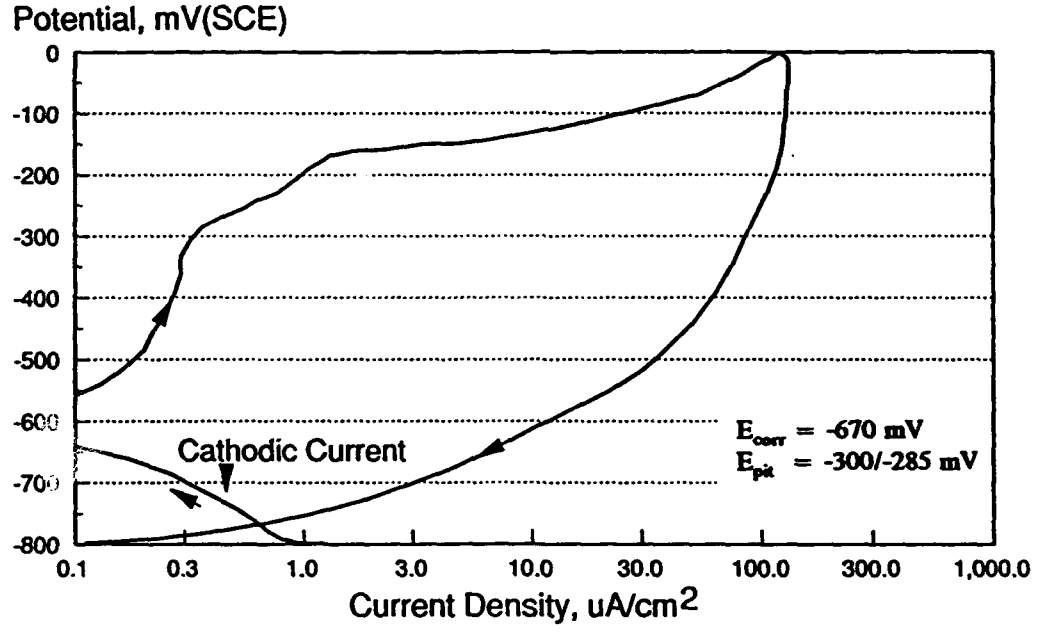


b. French Alloy

**Figure 10. Anodic polarization curves for four aluminum alloys (test environment: 100 ppm each of Cl, $SO_4$, and $HCO_3$ ions).**

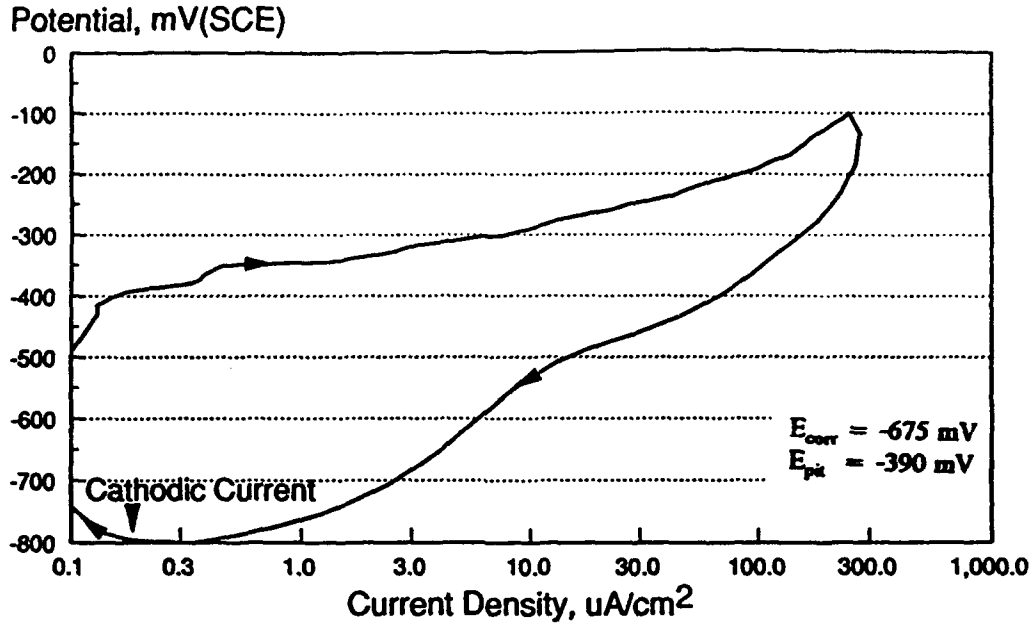


c. Alloy 2024-T3 (Anodized)

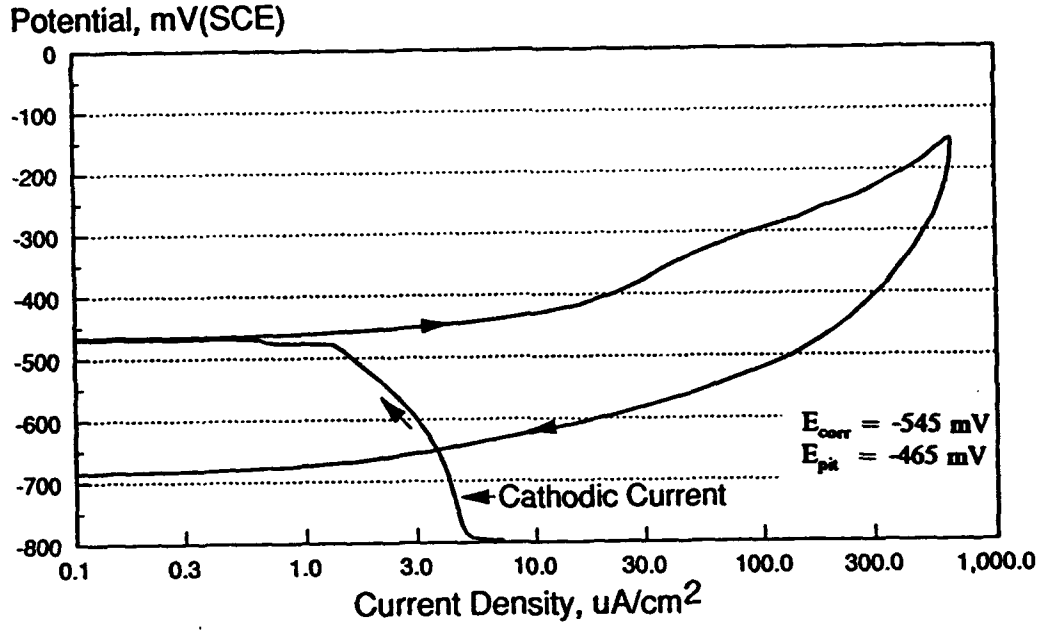


d. Alloy 2219-0

**Figure 10. (Continued)**

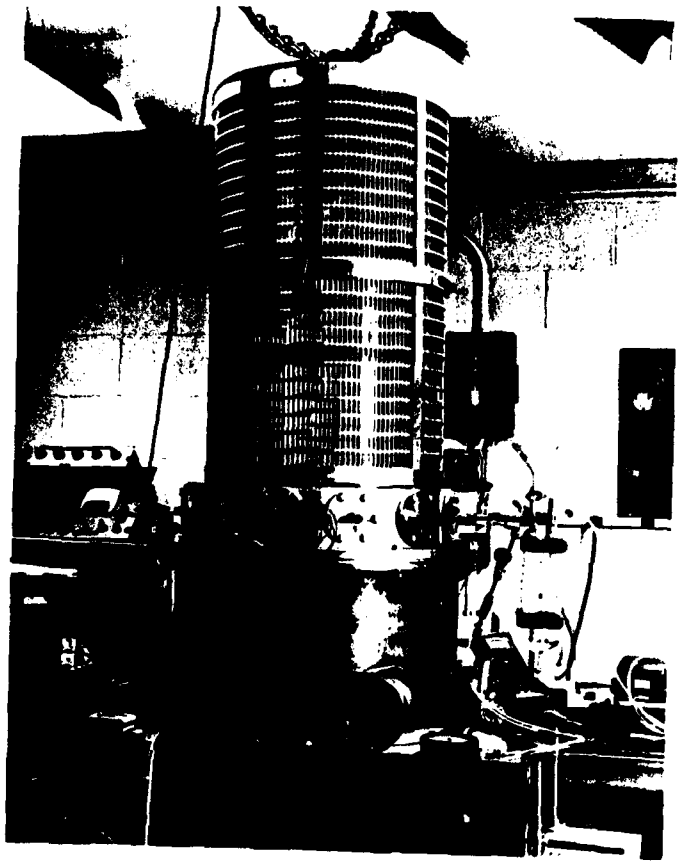

a. Vacuum Chamber

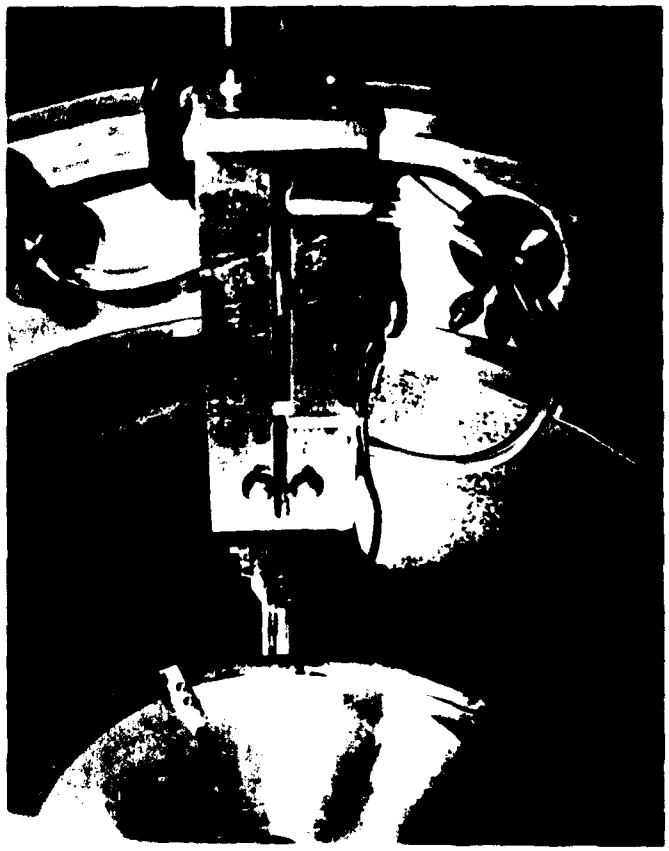

b. Aluminum Disc and Hypodermic Needle Assembly

Figure 11. High speed salt-bearing water test rig

The three-piece vacuum chamber is shown. The bottom section is a length of line pipe approximately 15 mm thick within which the aluminum disc is attached. Droplets are produced from an oscillating stream issuing from a hypodermic needle mounted to the assembly visible in (b).

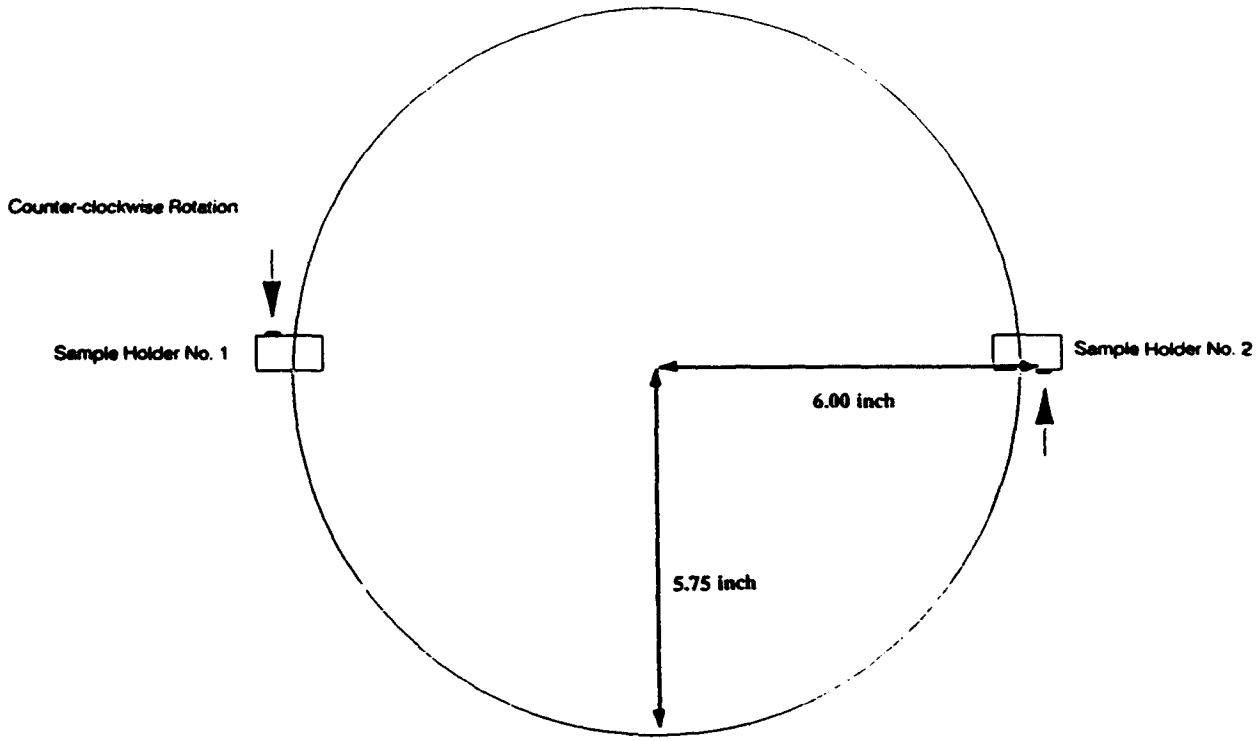


**Figure 12. Schematic drawing of disc and sample holder used in erosion testing device.**

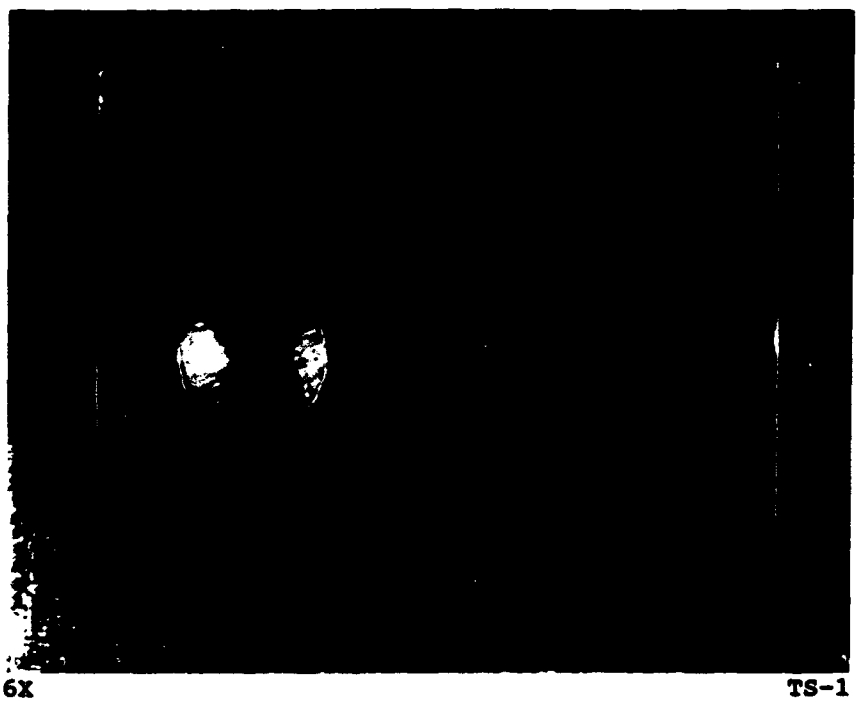


**Figure 13. Photograph documenting size and shape of test sample used during erosion testing.**

when the jet begins to neck down and pinch off into a drop under the action of surface tension. Any randomly occurring disturbance initiates instability; therefore, by introducing a high-amplitude periodic disturbance of an appropriate frequency the jet was made to pinch into drops at a very precise rate. The jet was issued from a hypodermic needle, sharpened and polished to minimize turbulent flow. A piezoelectric crystal oscillated the needle mount with an amplitude of only a few microns, which was sufficient to introduce nicely periodic Rayleigh instabilities. The optimal frequency for generating droplets depends upon flow rate and jet diameter. If V is the jet velocity and f the driven oscillation frequency, then the wavelength, $\lambda$, of the disturbance in the jet is simply V/f. Calibration tests indicated that optimal droplet generation resulted when $\lambda = 5d$, where d is the jet diameter. Salt- containing water droplets for impacting the samples were selected from the stream by either electrostatic manipulation or by a mechanical shutter.

The results obtained from the water droplet erosion testing performed on the "as-received" surfaces of all samples are provided in Table 7. Figures 14a through 14d document the progression of erosion-related damage on an unaged French alloy sample at four discrete exposure intervals. Additional photomacrographs of the "as-tested" condition of the individual samples after 12 hours of exposure to the salt-containing water droplets are provided in Appendix B.

Graphical summaries of the normalized weight-loss data collected for all materials tested during this task are provided in Figures 15a through 15d. These graphs assist in the interpretation of the data obtained for each material as a function of a fixed set of conditions that are representative of actual service conditions along the leading edges of the HU-25A wings. Testing was not designed to simulate the heated condition of these wing slats during anti-icing operation; therefore, all erosion tests were conducted at a constant temperature of 75°F.

The two sets of data plotted in Figure 15a document the erosion rates for both aged and unaged samples of Alloy 2219-0. A comparison among the data confirms that conditions used to artificially age the respective sample were significant enough to increase the inherent erosion resistance of this soft (Knoop hardness = 47) aluminum alloy. However, it was observed that the data collected after 12.5 hours of testing indicated that the inherent erosion resistance of this aluminum alloy was approximately six times less than the resistance measured for the French and 2024-T3 alloys. Examinations performed on both samples verified erosion-related perforations through the 0.043-inch-thick material after 12.5 hours of testing. This result along with the data

## Table 7. Results obtained from the water droplet erosion testing.

| Time (hours) | Normalised Weight Loss, mg/cm | | | | | | | | | | | | |
|---|---|---|---|---|---|---|---|---|---|---|---|---|---|
| | 2219-0 (Aged[1]) | 2219-0 (Unaged) | 2024-T3 (Aged[1]) | 2024-T3 (Unaged) | Hard Anodized 2024-T3 (Unaged) | French Alloy (Aged[2]) | French Alloy (Aged[3]) | French Alloy (Unaged) | French Alloy (Unaged) | French Alloy (Aged[4]) | French Alloy (Unaged) | French Alloy (Aged[4]) | French Alloy (Unaged) |
| 0 | 0 | 0 | 0 | 0 | 0 | 0 | 0 | 0 | 0 | 0 | 0 | 0 | 0 |
| 2.5 | 0.22 | 0.37 | 0.02 | 0.01 | 0.01 | 0.06 | 0.98 | 0.01 | 0.02 | 0.28 | 0.61 | 0.11 | 0.03 |
| 5.0 | 0.89 | 1.09 | 0.07 | 0.03 | 0.02 | 0.45 | 1.42 | 0.05 | 0.05 | 0.54 | 0.13 | 0.24 | 0.08 |
| 7.5 | 1.89 | 2.89 | 1.01 | 0.60 | 0.06 | 0.84 | 3.61 | 0.50 | 0.34 | 1.61 | 0.51 | 3.11 | 0.23 |
| 10.0 | 3.09 | 6.05 | 1.67 | 0.82 | 0.98 | 1.40 | 5.74 | 1.00 | 1.16 | 3.25 | 0.95 | 5.14 | 0.49 |
| 12.5 | 4.48 | 8.22 | 2.73 | 1.48 | 1.12 | 1.51 | 7.30 | 1.15 | 1.99 | 5.95 | 1.52 | 8.05 | 1.15 |

Notes:

(1) Aging Conditions: 24 hours at 204°C.
(2) Aging Conditons: Falcon Jet RH wing slat (>).
(3) Aging Conditions: Falcon Jet RH wing slat (N/A).
(4) Aging Conditions: 110 hours at 220°C.2.

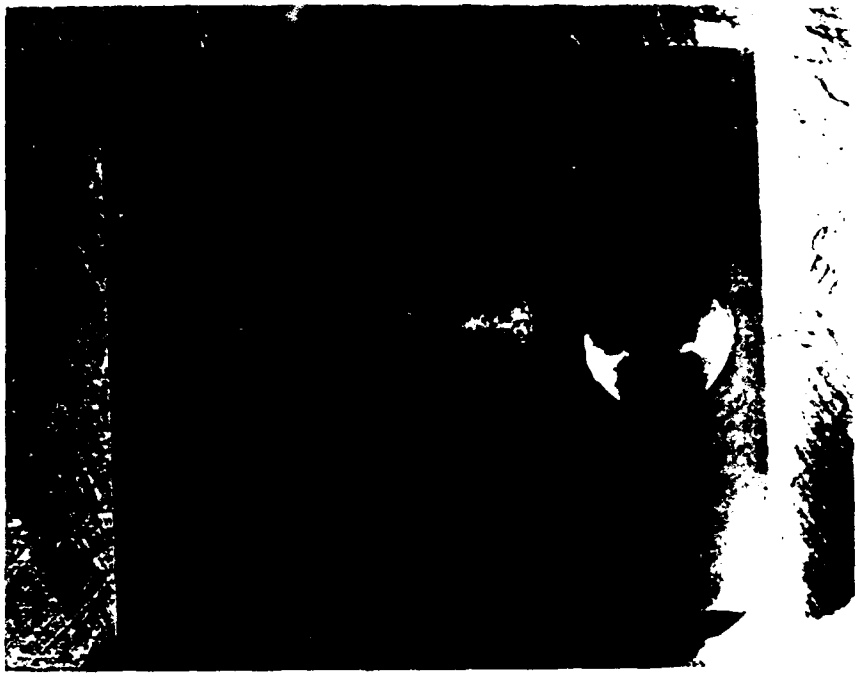

6X FA-1

a. 5 Hours

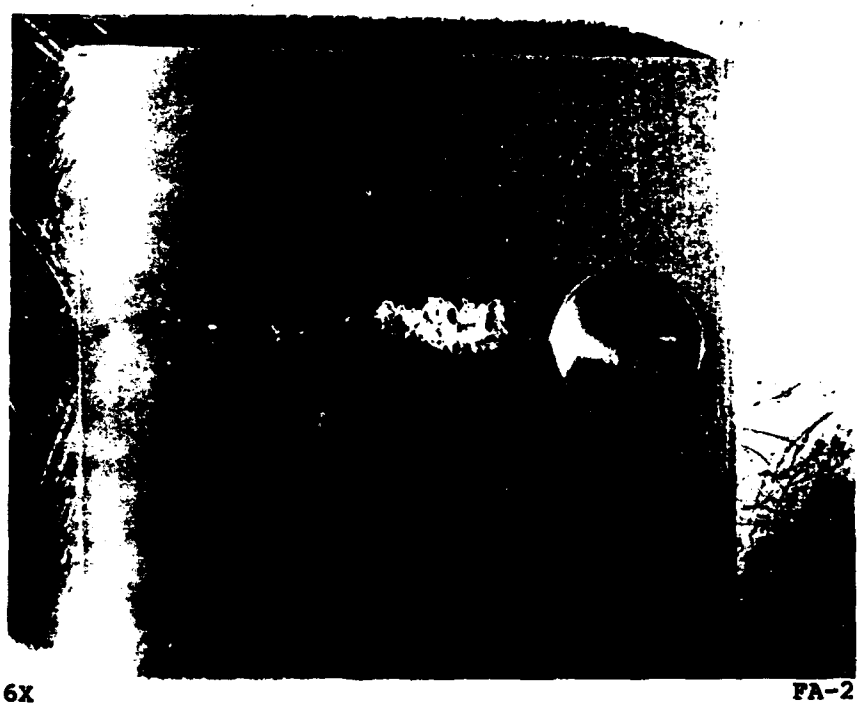

6X FA-2

b. 7.5 Hours

**Figure 14. Photograph documenting erosion damage occurring on unaged French Alloy at four exposure intervals.**

6X FA-3

c. 10 Hours

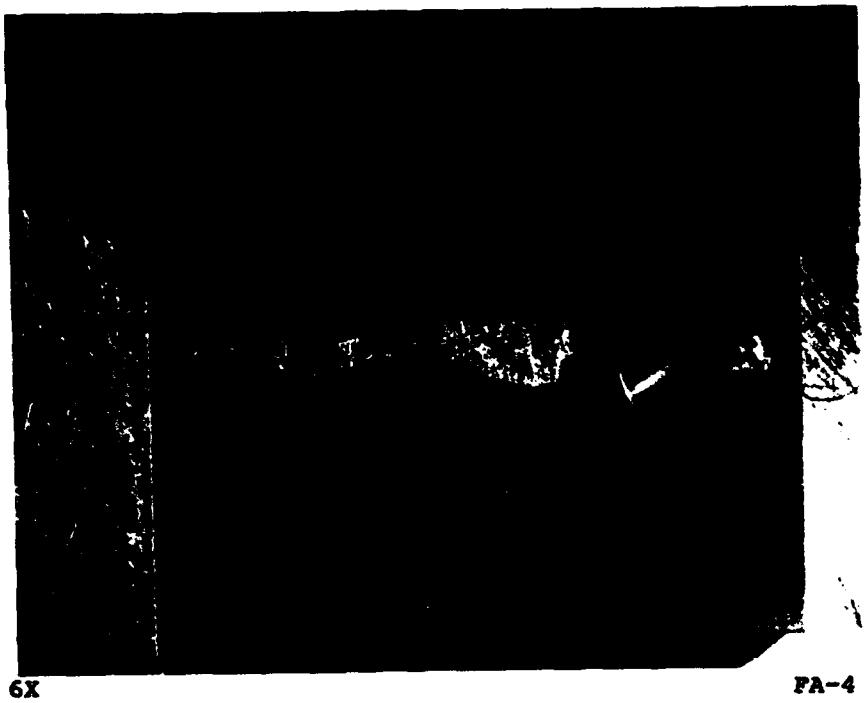

6X FA-4

d. 12 Hours

Figure 14. (Continued)

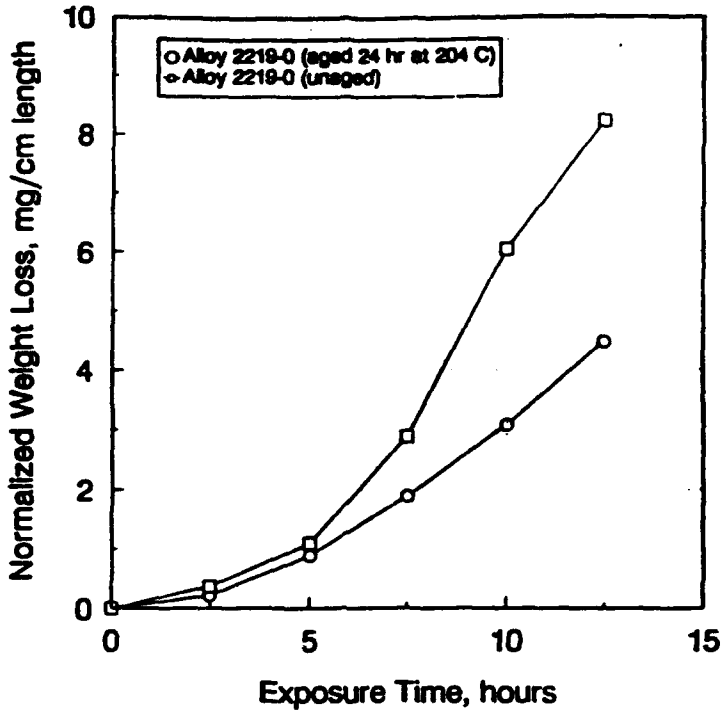


a. New and Aged Alloy 2219-0

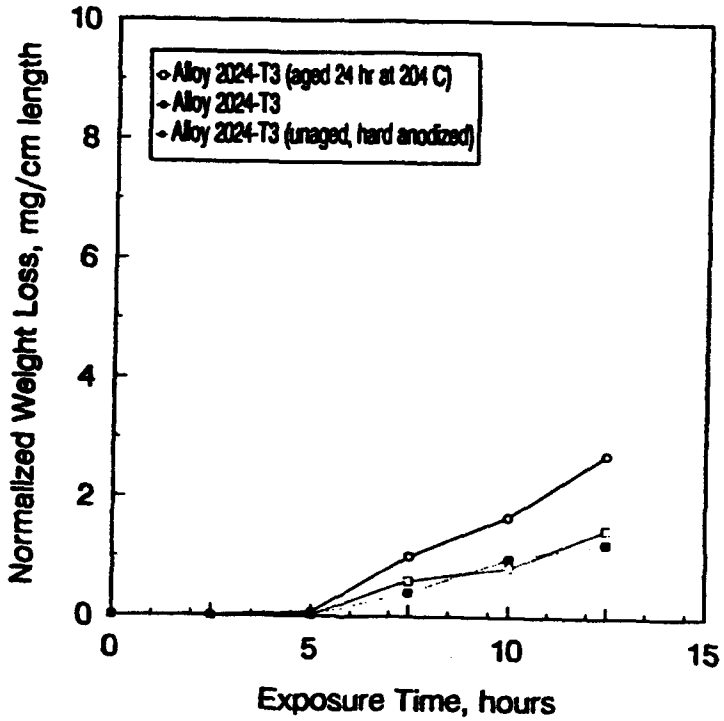


b. New, Aged, and Hard Anodized Alloy 2043-T3

Figure 15. Results of raindrop erosion tests performed on several aluminum aircraft alloys.

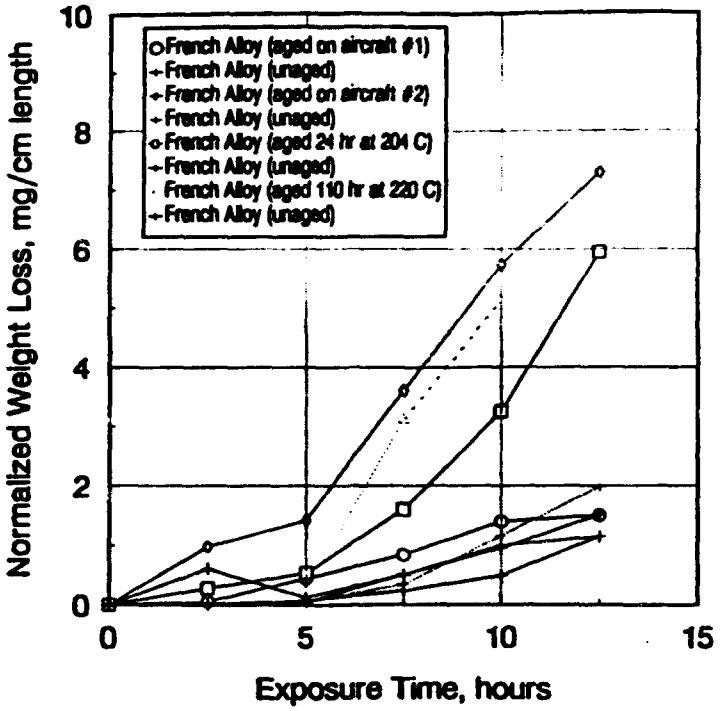


c. New and Aged French Alloy

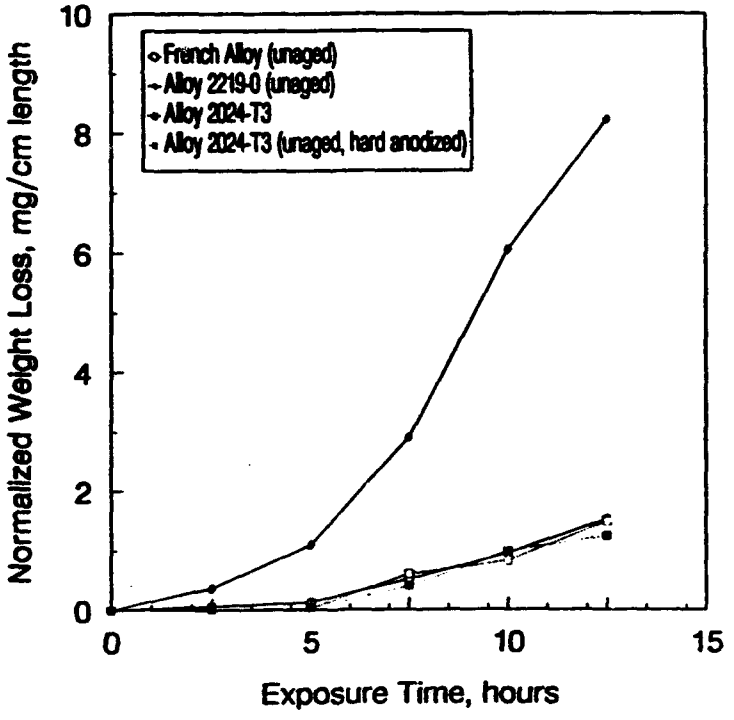


d. New French/2024-T3 and 2219-0 Alloys

Figure 15. (Continued)

obtained during Task 1 (poor corrosion resistance) confirms that this particular aluminum alloy should not be considered for use on the wing slats of the HU-25A aircraft.

Data presented in Figure 15b serve to illustrate the erosion-related performance between the aged (24 hours at 204°C), unaged, and unaged hard anodized (HA) Alloy 2024-T3 samples. The thick (0.0025 to 0.003 inch) anodic film on the test surface of the HA sample was produced to improve corrosion and erosion resistance of Alloy 2024-T3.

A comparison among the normalized erosion rates measured for the Alloy 2024-T3 samples after 12.5 hours of testing indicates that the artificially aged sample is approximately three times more susceptible to erosion damage than either of the other samples. The observed decrease in erosion resistance for this material may be attributed to grain boundary precipitation. This condition causes a decrease in the strength of the material, especially at the exposed surfaces of the sample, which also influences corrosion resistance. Specifically, the erosion results and the data collected for this material during the corrosion testing of Task 1 indicate that the overheating of the alloy will detrimentally influence erosion and corrosion resistance. However, it should be emphasized that the erosion damage measured on the French alloy that was aged to the same set of conditions was approximately two times as severe as the damage observed on the aged Alloy 2024-T3. This result strengthens the recommendation to select Alloy 2024-T3 as a replacement material for the French alloy.

The normalized rates measured for both the unaged (1) bare and (2) hard anodized Alloy 2024-T3 samples are almost identical. Pre-test examinations of the test surfaces of the hard anodized sample failed to reveal a crazing of the coating which is often associated with the growth of a thick anodic coating on aluminum alloys. The literature reports that this condition compromises the strength and erosion/corrosion resistance of the coating.

The unexpected low erosion resistance of the hard anodized Alloy 2024-T3 may be associated with the pretreated and/or pre-test surface roughness of the test sample. This condition is capable of causing a local spalling of the coating which adversely influences the resistance of the aluminum alloy to erosion and chemical attack. Gillig[14] has studied the effects of rain erosion at high velocity on the leading edges of aluminum aerofoils. Results indicated that failure depended primarily on the aluminum alloy being hard anodized. The best performance was obtained with 2024-T3 Alclad, 6061, and 2024-T3, in that order.

Spalling of the coating on Alloy 2024-T3 tested in the Battelle erosion rig was observed in a microscopic examination of the eroded areas on the test surface of the sample. No correlation between pre-test surface roughness and

the location of spalling damage on the unaged sample was performed during this task.

Figure 15c documents the normalized erosion rates measured for the French alloy samples. Data collected for the four unaged (control) samples indicates that the erosion test was reproducible. Normalized rates for this particular sample ranged between 1.01 and 1.99 mg/cm, with the average rate calculated at 1.41 mg/cm.

A comparison among the two naturally aged French alloy samples (removed from CG aircraft No. 1 and 2) and the two artificially aged samples confirms the following:

(1) Susceptibility to erosion damage was highest for the samples that were removed from the overheated and discolored leading edge section of a center wing slat from aircraft No. 2 and the sample that was artificially aged at 220°C for 110 hours.

(2) The measured erosion resistance and measured level of damage on the sample that was artificially aged for 24 hours at 204°C was slightly higher than that measured for the sample removed from aircraft No. 2.

(3) The magnitude of damage measured for the two artificially aged samples and the sample removed from the overheated wing section of aircraft No. 2 confirms that the most severe damage accelerated after five hours of testing.

(4) Heating of the sample removed from an area approximately 10 inches from the overheated wing section of aircraft No. 1 (T/N 2131, MY2014730G01SN159F) was not sufficient to induce an adverse transformation of the French alloy's microstructure. The erosion resistance of this naturally aged sample was comparable to the unaged French alloy samples.

The results obtained from the above mentioned comparisons confirm that the conditions (24 hours at 204°C) selected to artificially age the aluminum alloys investigated during this task were adequate based on the limited data available for the field retrieved (naturally aged) samples. Specifically, the length of time each sample was exposed to the overheating (antiicing) condition. The data suggest that an ideal set of aging conditions may have been 110 hours at 220°C.

A comparison among the four unaged samples tested during this task is provided in Figure 15d. The data indicate that the erosion-related performance of the hard anodized and bare Alloy 2024-T3 samples and the French alloy is equivalent. As stated in the previous text, the rate of erosion increased after 5 hours of exposure testing. Conversely, the data collected for Alloy 2219-0 suggest that this aluminum alloy should not be considered as a candidate replacement material for the outer wing slats of the HU-25A aircraft. The same conclusion was obtained from the corrosion testing conducted on this material.

## Task 3. Wing Slat Temperature Evaluation

Two sets of eight-dot (eight discrete temperature ratings) nonreversible temperature labels were ordered from Omega® Engineering and used in this task to determine the temperature obtained on the internal surfaces of the center wing slat during antiicing conditions. Each label contained a total of eight indicator dots, which turned black at the rated temperatures identified on the respective label. A listing of the two types of labels and corresponding temperature ratings specified for each label used in this task is provided in Table 8.

**Table 8. Non-Reversible Temperature Labels Used in Task 3.**

| Model No. | Temperature Range, F | | | | | | | |
|---|---|---|---|---|---|---|---|---|
| TL-E-330 | 330 | 340 | 350 | 360 | 370 | 380 | 390 | 400 |
| TL-E-410 | 410 | 420 | 435 | 450 | 465 | 480 | 490 | 500 |

Placement of each pair of labels (0.75-inch wide by 2.0-inches long) along the wing slats of two operational Falcon Jet aircraft stationed at the Coast Guard Aircraft Repair Service Center (ARSC) in Elizabeth City, N.C., was performed by Coast Guard personnel. The Program Manager at the Coast Guard R&D Center and representatives from the Falcon Jet Corporation were consulted on the selecting a service exposure period which would ensure that the highest possible temperatures along the wing slat were obtained.

The results obtained from the initial exposure of the temperature labels at ARSC indicated that the temperatures along the internal surfaces of the center wing slat were lower than 330°F. As a result, the temperature sensitive dots were unable to detect and record the precise temperatures of the aluminum wing slat. It was concluded that the temperature measurements were affected by the in-flight flow of air across the leading edges of the center wing slat. This airflow pattern caused a significant decrease in the metal temperature that was measured.

In response to the results obtained from the initial exposure, an additional set of temperature labels were installed on a single aircraft in the locations shown in Figure 16. The temperature range of these labels was 200 to 400°F. All labels were installed into the same areas as the initial set of labels. The results collected by the second set of labels indicated that the temperatures along the center wing slat were between 285 and 320°F. Coast Guard and Falcon Jet personnel stated that these temperatures may be slightly lower than the actual skin temperatures because of the air flow condition.

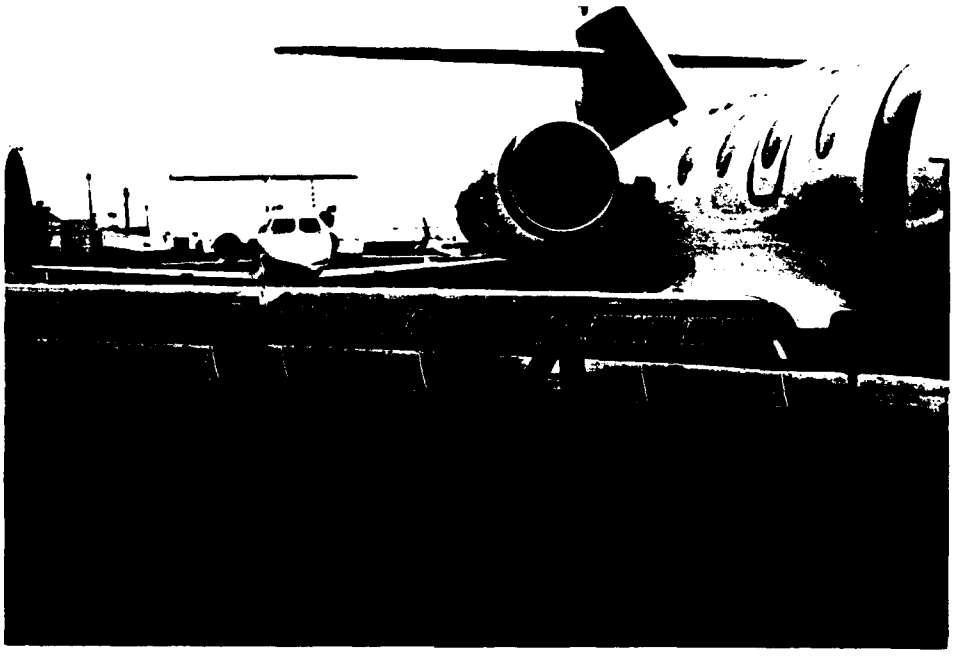

a. LH Wing

b. Area of overheating and/or discoloration on center wing slat

Figure 16. Photographs documenting approximate placement of temperature labels on inboard and center wing slats of HU-25A Falcon jet.

Efforts to obtain more accurate temperature measurements using thermocouples attached to the internal surfaces of the center wing slat were abandoned with the transfer of Coast Guard personnel at ARSC.

## Task 4. Literature Search

The operating environments of aircraft in the collective Coast Guard fleet vary widely, as does the susceptibility of each type of aircraft to corrosion. Unlike stationary structures, the level of corrosion occurring in and/or on aircraft varies as a result of several factors, not the least of which is the fact that in flight the aircraft experiences widely varying conditions as a result of geographical location, range, altitude, and weather changes. A considerable amount of an aircraft's service time is spent on the ground; therefore, the environment of the base or installation responsible for maintenance, readiness, and reliability is an important consideration.

The objective of this task was to conduct a literature search of available technical articles for the purpose of determining the effects of distance from the ocean (salt air) on Coast Guard aircraft corrosion. The search included a review of proceedings from several symposia sponsored by the American Society for Testing and Materials (ASTM) Committee G-1 on Corrosion of Metals. The majority of the published papers contained the protocol and results of laboratory and/or field testing that was performed for the purpose of obtaining atmospheric corrosion information on both ferrous and non-ferrous materials. Technical papers authored by international experts were also obtained and reviewed in an effort to validate the corrosion data presented in each of the ASTM articles.

Accelerated corrosion near the ocean is correlated with airborne sea salt, but establishing a critical distance from the shore is difficult because there is a limited amount of quantitative information relating corrosion to atmospheric salt concentrations, or even relating salt concentrations to distance from the shore. The chlorides in salt spray are primarily responsible for an aggravation of aircraft corrosion in ocean environments. This statement is supported by studies conducted by Ambler and Bain[1] in Nigeria and also Ailor[2] in the United States. Both studies included specimens of steel and aluminum that were exposed at distances from the ocean ranging from a few yards to over 100 miles. The concentration of salt particles in the atmosphere at the various test locations was measured in an effort to characterize the magnitude of damage by the level of chlorides. Results obtained from the studies indicated that samples closest to the ocean corrosion had almost ten times the corrosion rate of those approximately 500 yards away from the ocean.

Larger salt particles settle from the air rapidly; whereas, small particles persist in the atmosphere and serve as condensation points for rainwater. Thus, any detectable level of chlorides in rainwater over land masses is correlated with small particles. Junge and Gustafson[3] reported a direct settling of large particles occurs near the sea shore. Additionally, it is unlikely that the presence of chlorides in rainwater is relevant to corrosion because the decrease of chloride content in rainwater occurs over large distances, but the measurable decreases in corrosion damage are significant (Hudson and Stanner[4]). Corrosion rates at a 6.2-mile distance from the shore are approximately the same as corrosion rates far inland. Consequently, a critical proximity to the sea should be determined not from the rainwater chloride concentration, but from particulate chloride concentrations.

Similar results were obtained by Coburn[5] in a series of atmospheric tests that were conducted at the Inco marine atmospheric corrosion test station at Kure Beach, North Carolina. Materials tested at this test site included steel, zinc, and aluminum. Post-exposure weight loss data indicated that there was an eightfold reduction in the corrosivity of the atmosphere related to a lower concentration of airborne salt 800 feet from the ocean as compared with 80 feet. Sowinski and Sprowls[6] obtained a similar correlation between distance from the ocean and corrosion of numerous wrought and cast aluminum alloys that were exposed at Alcoa marine test sites located throughout the United States.

The corrosivity index of Coast Guard installations located in marine environment may vary widely as a consequence of several factors. One important factor includes the direction of prevailing winds relative to the ocean and the topography of the shoreline which affects wave action and the amount of salt particles thrown into the air by the surf. Waves either pound a rocky shore or remain still on a wide gentle beach. The effects of both conditions and their impact on corrosion were illustrated by marine atmospheric corrosion tests conducted by the American Society for Testing Materials at LaJolla, California, and Key West, Florida.[7] Corrosion rates measured for various steel and aluminum alloys indicated that the former location was more corrosive than the latter as a result of continuous exposure to air saturated with sea salt. The Key West location, which was adjacent to a calm lagoon, was even less corrosive than the inland atmosphere at State College, Pennsylvania.

Additional factors that influence the corrosion rates of the aluminum alloys being investigated in this program include the level of rainfall, temperature, and humidity in the marine environment. McGeary et al.[7] found that in the presence of a given hygroscopic salt, corrosion will not occur

until the relative humidity exceeds a certain value, which is dependent on the identity of the salt. For sodium chloride (NaCl), this value is 78 percent RH at 20°C, and with increasing temperature the relative humidity value is decreased (75 percent at 25°C). Rain promotes corrosion by providing moisture and washing away soluble corrosion products. Rain also retards corrosion by washing away pollutant and salt air deposits.

In summary, the limited information obtained during this task suggests that salt concentrations and corrosion rates for steel and aluminum materials decrease monotonically to approximately 1 mile, with most of the decrease occurring within 800 yards. Corrosion rates and salt concentrations remain constant between 1 and 6.2 miles, unless other pollutants and/or environmental factors are considered.

## SUMMARY OF RESULTS

The following results were obtained from this program:

(1) Microhardness measurements indicate that the average hardness values for Alloy 2219-0, Alloy 2024-T3, and the French alloy were 47, 137 and 153, respectively. The hardness of the naturally aged French alloy sample retrieved from aircraft No. 1 was 150.5.

(2) Microstructural analyses confirmed that the hole on the damaged leading edge of a center wing slat of aircraft No. 1 (T/N 2131) developed in response to (1) local microstructural changes resulting from a hot air antiicing system, and (2) the operating environment of the aircraft which promoted corrosion and rain drop erosion damage.

(3) Bulk analyses confirmed that the concentrations of various alloying elements in the Alloy 2024-T3 and Alloy 2219-0 samples are consistent with the specifications listed in the ASM Handbook. Additionally, the higher concentrations of several elements (Si, Cu, and Mn) in the French alloy are within the specified ranges for the elements in Alloy 2024-T3.

(4) The microstructure of the French alloy aged for 12 hours at 246 C was similar to the microstructure of the French alloy sample retrieved from a damaged (overheated) section of aircraft 2131.

(5) Corrosion testing indicates that the corrosion resistance of aged/unaged Alloy 2024-T3 and French alloy samples are identical. By comparison, the resistance of Alloy 2219-0 was poor.

(6) Retempering of Alloy 2219-0 increases erosion resistance; however, the measured resistance is approximately six times less than that measured for the French and 2024-T3 alloys.

(7) Normalized erosion rates for the unaged (1) bare and (2) hard anodized Alloy 2024-T3 are identical. The pre-test surface roughness of the hard anodized material may restrict superior performance. Silicone wax or sealants should be used to improve material performance in a corrosive marine environment.

(8) The erosion resistance of the two naturally aged French alloy samples removed from two CG aircraft varied as a result of the length of time each sample was exposed to the antiicing temperatures and corrosive operating environment.

(9) A review of available literature suggests that there is an eight- to ten-fold reduction in the level of corrosivity between 80 and 800 yards from the ocean, as measured on steel and aluminum specimens. Prevailing winds and shoreline topography must be considered.

(10) Corrosivity of a marine environment decreases monotonically to approximately 1 mile, and remains constant through 6.2 miles. Industrial pollutants and/or adverse environmental factors must also be considered.

## CONCLUSIONS

(1) Inferior corrosion and erosion resistance restricts the use of Alloy 2219-0 as a candidate replacement alloy for the outer wing slats of the HU-25A aircraft.

(2) The literature suggests that the corrosion resistance of the hard anodized 2024-T3 alloy is excellent. This condition is desirable for wing slat application; however, additional corrosion testing of aged samples must be performed before this material is recommended in place of Alloy 2024-T3.

(3) Airflow across the leading edges of the outer wing slats of an HU-25A aircraft during antiicing decreased metal temperatures; therefore, limiting the ability to obtain an accurate temperature measurement using temperature indicating labels. The measured temperatures are lower than the actual skin temperatures because of the airflow condition.

## REFERENCES

(1) Ambler, A.W., and Bain, A.A., Journal of Applied Chemistry, 5 (Septemb. 1955).

(2) Ailor, W.H., Jr., "Performance of Aluminum Alloys at Other Test Sites," Metal Corrosion in the Atmosphere, ASTM STP 435, American Society for Testing and Materials, pp. 285 -307 (1968).

(3) Junge, C.E., and Gusyafson, R., "On the Distribution of Seas Salt Over the United States and Removal by Precipitation," Tellus, 9, 164 (1957).

(4) Hudson, J.C., and Stanner, J.F., Journal of Iron and Steel Inst., 180, 271 (1955).

(5) ASTM, "Corrosiveness of Various Atmospheric Test Sites as Measured by Specimens of Steel and Zinc," Metal Corrosion in the Atmosphere, ASTM STP 435, pp. 360 - 391 (1968).

(6) Sowinski, G., and Sprowls, D.O., "Weathering of Aluminum Alloys," Atmospheric Corrosion, pp. 297 - 328 (1982).

(7) Tracy, A.W., ASTM Special Technical Publication 175, p. 67 (1956).

(8) McGeary, F.L., Summerson, T.J., and Ailor, W.H., Jr., "Atmospheric Exposure of Non-Ferrous Metals and Alloys - Aluminum; Seven-Year Data, " Metal Corrosion in the Atmosphere, ASTM STO 435, American Society for Testing and Materials, pp. 141 - 174 (1968).

(9) Duncan, J.R., and Ballance, J.A., "Marine Salts Contribution to Atmospheric Corrosion," Degradation of Metals in the Atmosphere, ASTM STP 965, S.W. Dean and T.S. Lee, Eds., American Society for Testing and Materials, pp. 316 - 326 (1988).

(10) Carter, V.E., "Atmospheric Corrosion of Aluminum and Its Alloys: Results of Six-Year Exposure Tests," Metal Corrosion in the Atmosphere, ASTM STP 435, American Society for Testing and Materials, pp. 257 - 270 (1968).

(11) Aircraft Corrosion, AGARD Conference Proceedings No. 315, Proceedings of a Conference held at Cesme, Turkey, 5-10th April 1981.

(12) Bailey, J.C., Porter, F.C., and Pearson, A.W., Aluminum and Aluminum Alloys, in Corrosion, Vol. 1, Chapter 4, Edited by L.L. Schrier, Newnes-Butterwoths Press, London and Boston, 1977.

(13) Aluminum Properties and Physical Metallurgy, edited by J.E. Hatch, American Society for Metals Publication (1984).

(14) Gillig, F.G., "Study of Hard Coatings for Aluminum Alloys," W.A.D.C. Technical Report 53 - 151, P.B. 111320 (1953).

# Appendix A

## Photographs Documenting Post-Test Condition of Aluminum Alloys Exposed to ASTM B117-85 Salt Fog Corrosion Test

**Artificial Aging Condition No. 1**

- **Heat to 300 F for 24 hours**
- **Air cool to 76 F**

Alloy 2219-0 (Bare)

Alloy 2024-T3 (Chromated)

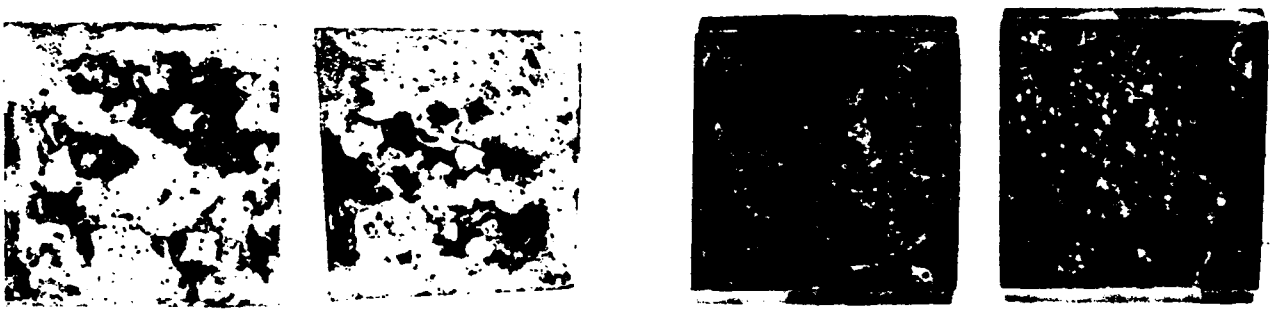

Alloy 2024-T3 (Bare)

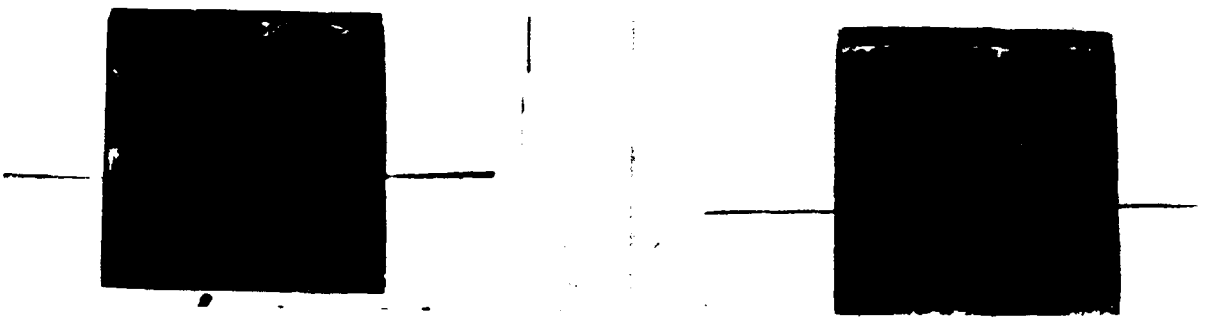

French Alloy (Chromated)

As-Tested

As-Cleaned

**Artificial Aging Condition No. 2**

- **Heat to 475 F for 12 hours**
- **Air cool to 76 F**

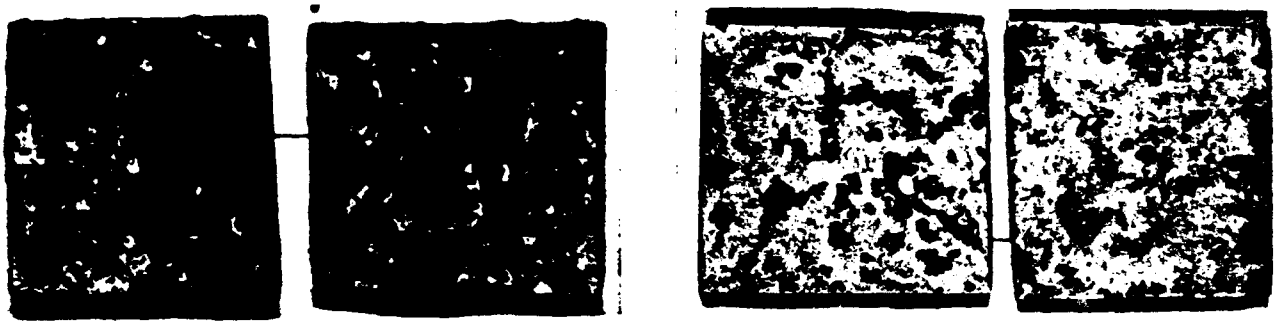

Alloy 2219-0 (Bare)

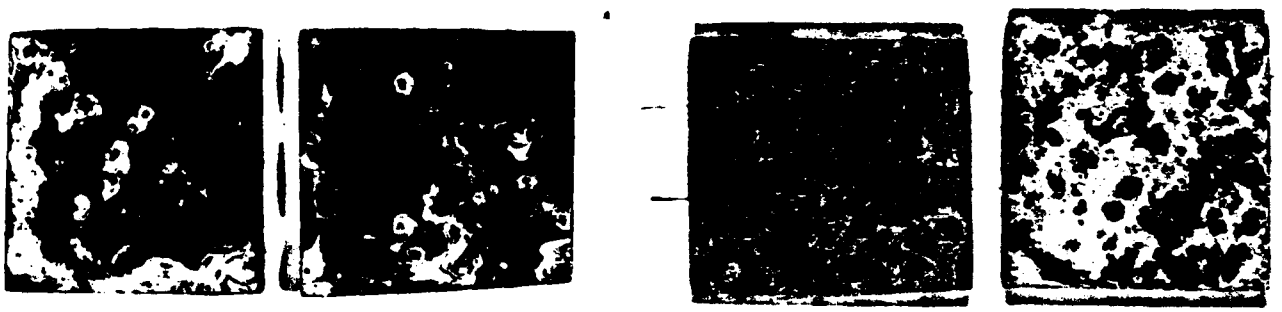

Alloy 2024-T3 (Chromated)

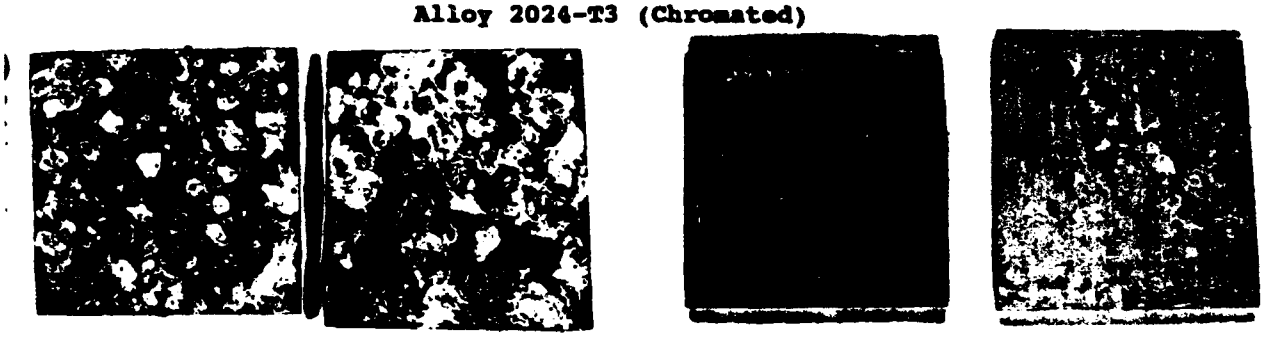

Alloy 2024-T3 (Bare)

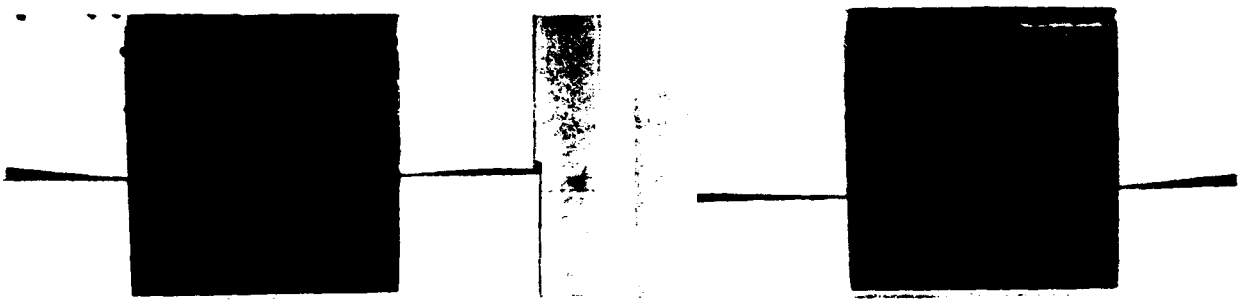

French Alloy (Chromated)

As-Tested

As-Cleaned

**Artificial Aging Condition No. 3**

- **Heat to 300 F for 4 hours**
- **Air cool to 76 F**
- **Repeat cycle 2 times**

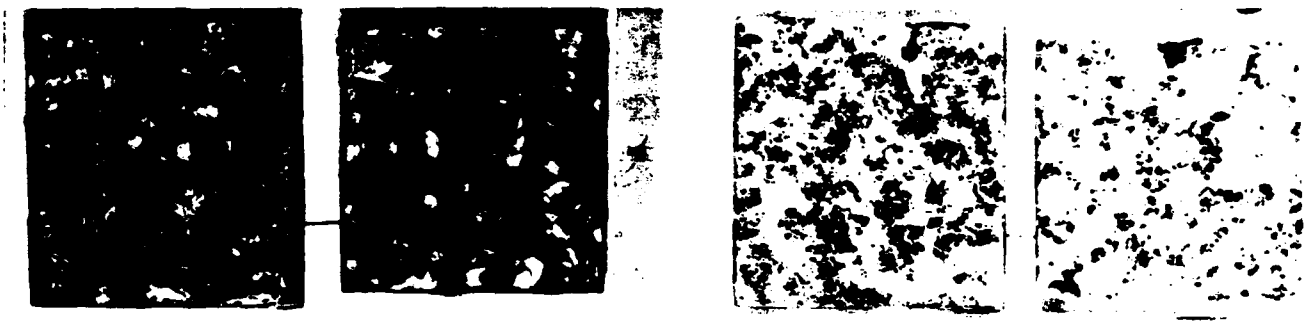

Alloy 2219-0 (Bare)

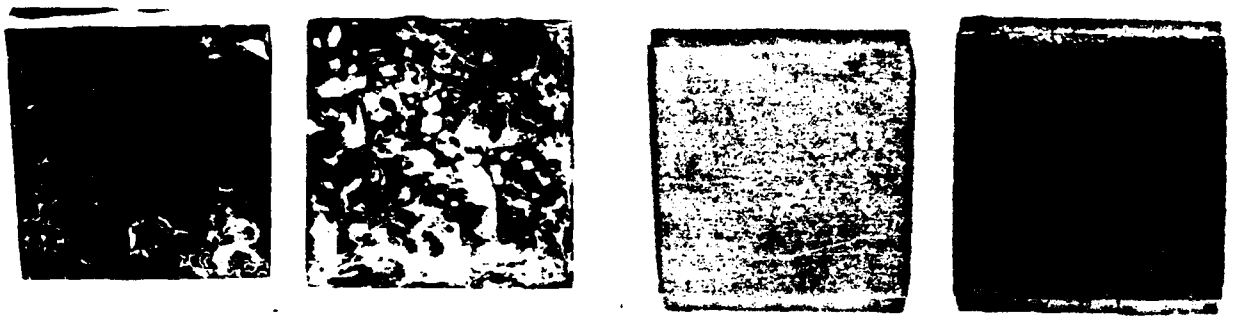

Alloy 2024-T3 (Chromated)

Alloy 2024-T3 (Bare)

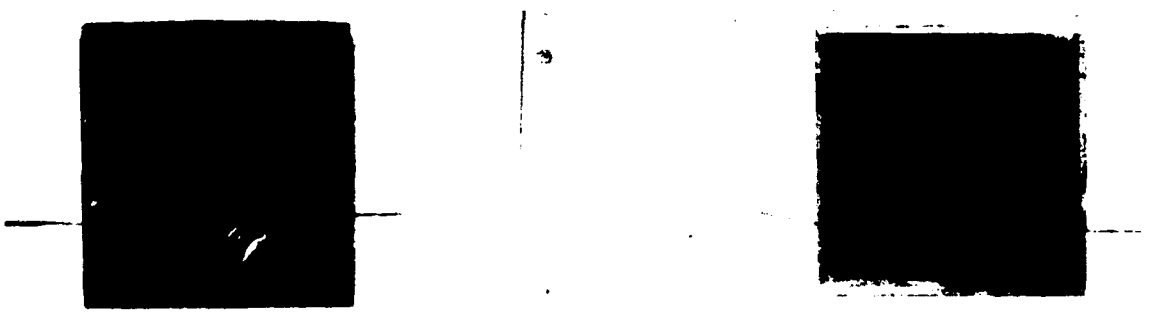

French Alloy (Chromated)

As-Tested

As-Cleaned

# Appendix B

## Photographs Documenting the "As-Tested" Condition of Aluminum Alloys Exposed to Raindrop Erosion Test

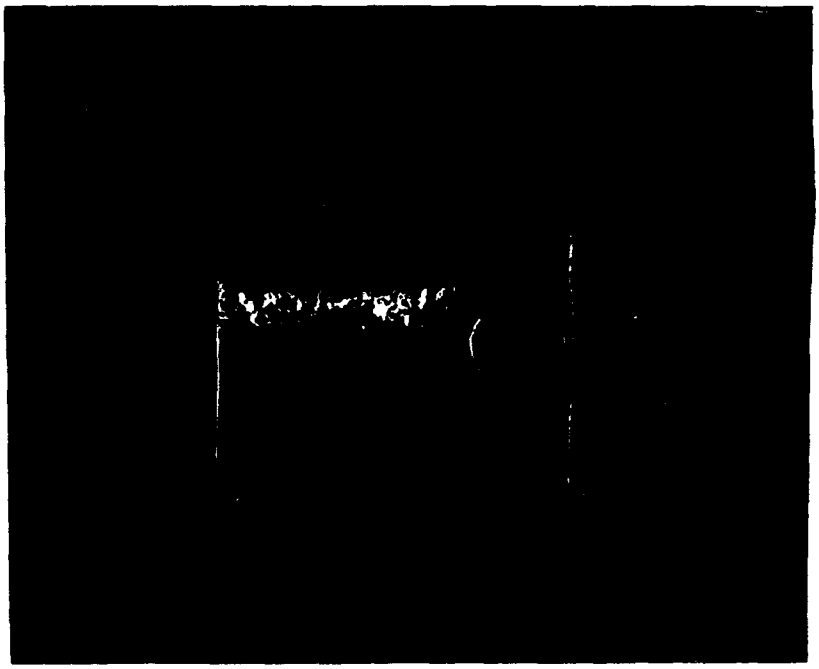

3.5X B1

Alloy 2219-0 (Unaged)

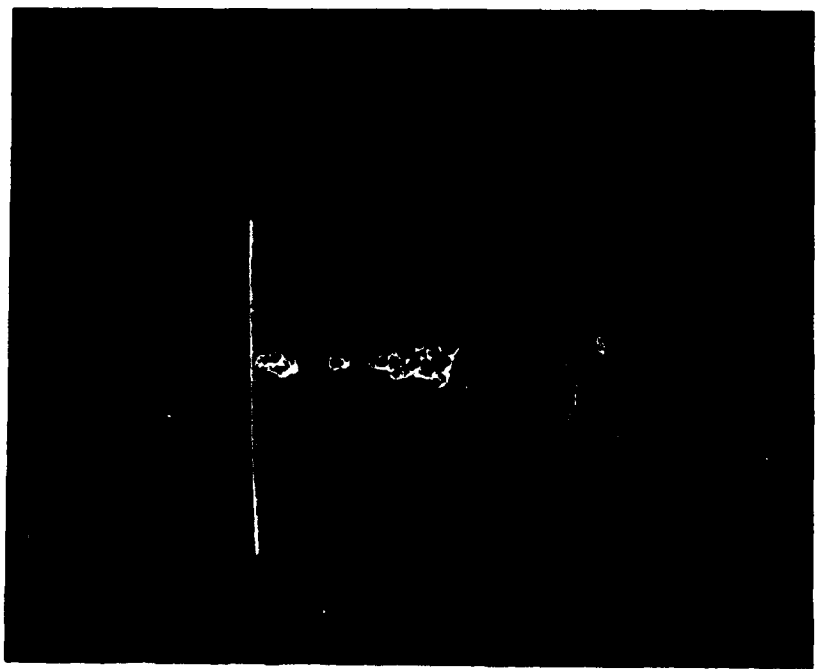

3.5X B2

Alloy 2219-0 (Aged)
(24 hrs at 204 C)

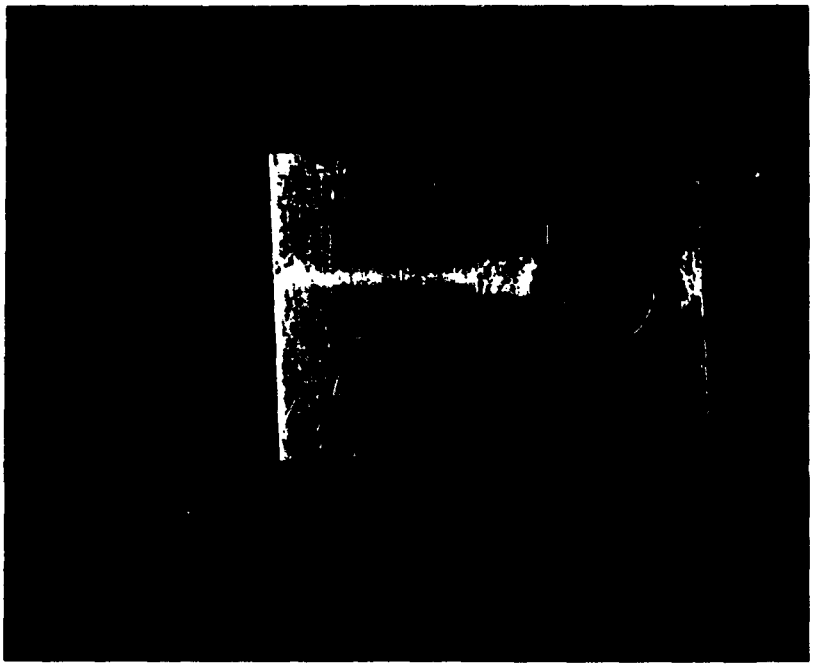

3.5X B3

Alloy 2024-T3 (Unaged)

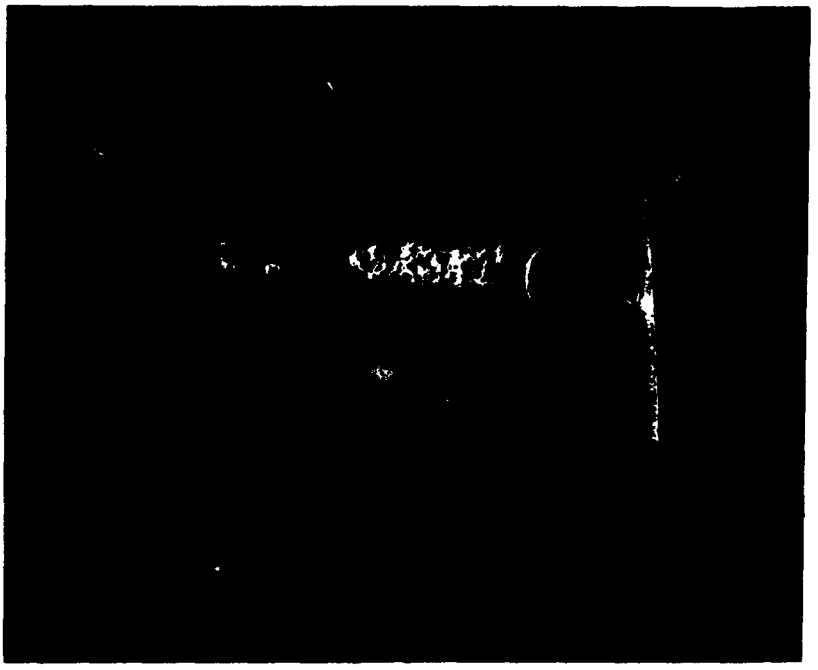

3.5X B4

Alloy 2024-T3 (Aged)
(24 hrs at 204 C)

3.5X B5

French Alloy (Unaged)

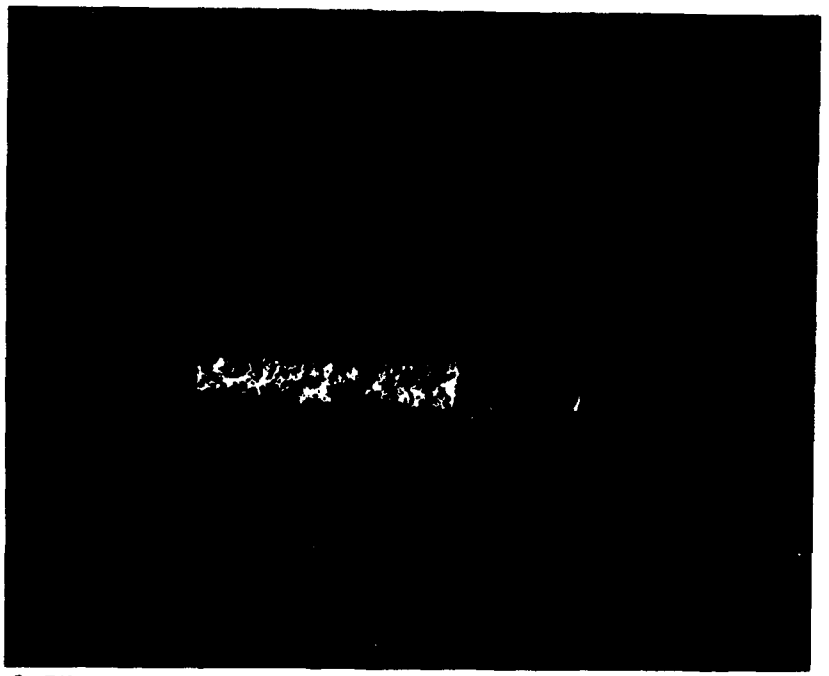

3.5X B6

French Alloy (Aged)
(24 hrs at 204 C)

3.5X B7

French Alloy (Aged)
(A/C No. 1)

3.5X B8

French Alloy (Aged)
(A/C No. 2)

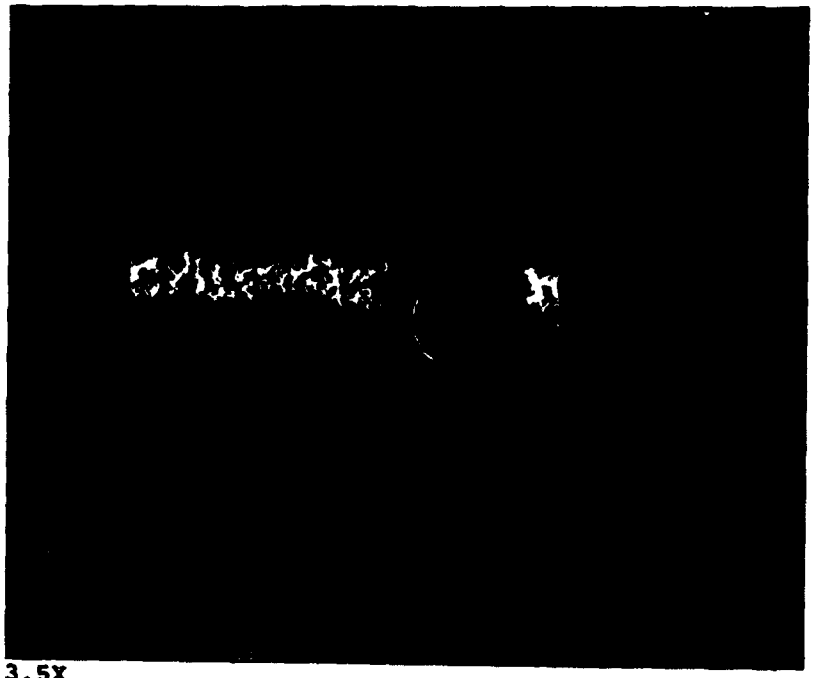

3.5X B9

French Alloy (Aged)
(110 hrs at 220 C)

3.5X B10

Alloy 2024-T3 (Unaged)
(Hard Anodized)